Gulf of Mexico Hydrate Mapping and Interpretation Analysis

Phase-II, Project Area 2.1 Report

Aditya Kumar, Alexey Portnov, Ann Cook

June 30, 2023

This report satisfies Mapping and Prospect Identification within Project Area 2.1 for BOEM award Gulf of Mexico Gas Hydrate Mapping and Interpretation Analysis, which is Deliverable/Milestone 4.

Table of Contents

1 Study Area and Data 2
2 RMS Mapping 5
3 Classification of BSRs 6
4 Results in Project Area 2.1 6
4.1 Zone 1 6
4.2 Zone 2 15
4.3 Zone 3 22
4.4 Zone 4 27
4.5 Zone 5 30
4.6 Zone 6 33
5 Gas resource estimation 36
6 Conclusion 37
7 References 38

Table 1. List of required deliverables and figures.

Sr.	Deliverable	Figure #
1	A map showing the spatial distribution of BSRs within Project Area 2.1	2
2	Regional seismic cross sections showing the base of gas hydrate stability and the relationship of prospective reservoir intervals to channel levee systems, faults, salt, and other geologic features.	4-8, 11 -17, 19-24, 26-27, 29-30, 32-34
3	RMS amplitude maps that correlate with the identified BSR zones	10, 18, 25, 28, 31
4	Correlation of well logs and seismic data	5-8, 11

1 Study Area and Data

Project Area 2.1 covers approximately 15,800 km^2 and includes the eastern part of the East Breaks protraction area, the western part of the Garden Banks protraction area, and a small part of the northern Alaminos Canyon protraction area (as illustrated in Figure 1a). The water depth within this area varies from 100 to 1700 meters (as shown in Figure 1b). Areas with a water depth less than 500 meters lie outside the methane hydrate stability zone (Figure 2).

For Project Area 2.1, we used fourteen seismic surveys available at the National Archive of Marine Seismic Surveys (NAMSS; Triezenberg et al., 2016) database (Figure 1a). These surveys cover 82% of Project Area 2.1.

In Project Area 2.1, we have identified a total of ten bottom-simulating reflections (BSRs) which were categorized into six distinct zones (Figure 2). The shallowest BSR is mapped at 780 m water depth within Zone 3. A majority of these BSRs are associated with salt ridges, domes, and their flanks. This pattern of BSR occurrence over salt structures has been observed in other regions of the northern Gulf of Mexico (Portnov and Cook, 2019, 2020; Skopec et al., 2021). Among the ten BSRs, three were not identified by the Bureau of Ocean Energy Management (BOEM) in previous work (e.g. Shedd et al., 2012).

Several wells have been drilled within Project Area 2.1, and a few of these wells penetrate the mapped BSRs as shown in Figure 2. The well log data was acquired from the Bureau of Safety and Environmental Enforcement (BSEE) database and the Lamont-Doherty Joint Industry Program (JIP) logging database. The well logs were integrated with seismic data to gain insights into the fluid content, porosity, sediment type, and possible hydrate or natural gas occurrence within and below the hydrate stability zone.

Microbial gas hydrates were recovered in piston cores at five locations within Project Area 2.1 (Sassen et al., 2001) (Figure 2). Only one of these five locations coincides with a BSR zone (Figure 2).

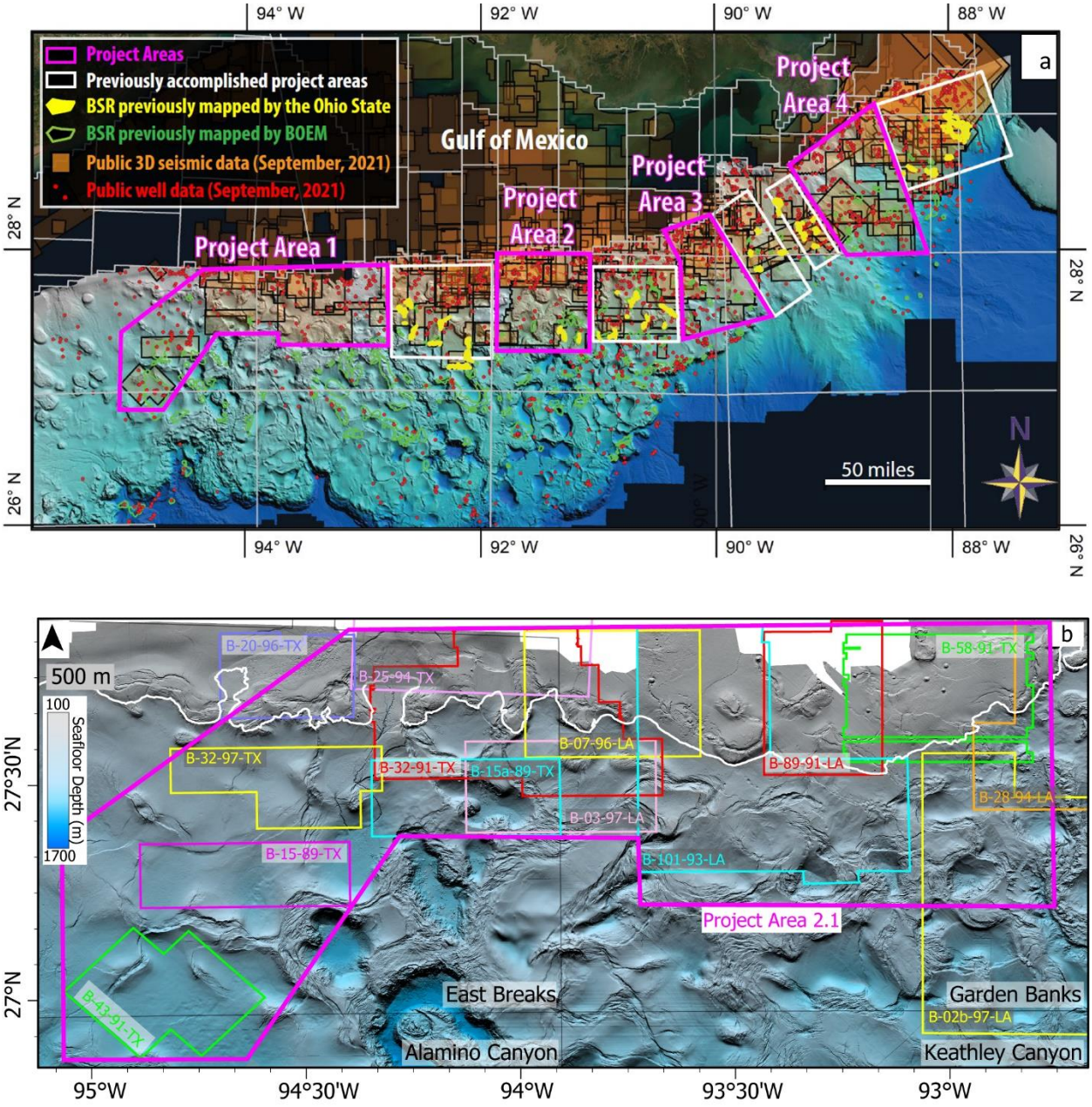

Figure 1: a) A regional bathymetry map of the northern Gulf of Mexico (Kramer and Shedd, 2017) showing Project Areas of Phase 1 (white squares) and Phase 2 (pink squares). b) Project Area 2.1 and the outline of each seismic survey used in this report.

	Survey name/BOEM identifier	Year	Area of seismic survey (km^2)	Frequency Range (Hz)	Survey quality	Bin size (m)	Projection
1	B-101-93-LA/L93-101	1993	2900	8-80	Poor	20×12.5	15N NAD 1927, feet
2	B-89-91-LA/L91-089	1991	1000	5-100	Poor	20×12.5	15N NAD 1927, feet
3	B-58-91-LA/L91-58	1991	1350	5-80	Poor	22.8×15.2	15N NAD 1927, feet
4	B-28-94-LA/L94-028	1994	600	5-80	Poor-Fair	20×12.5	15N NAD 1927, feet
5	B-07-96-TX/T96-007	1996	1327	5-75	Poor-Fair	25×25	15N NAD 1927, feet
6	B-03-97-TX/T97-03	1997	1000	5-80	Poor-Fair	15×12.5	15N NAD 1927, feet
7	B-02b-97-TX/T97-02b	1997	1100	5-65	Fair	20×12.5	15N NAD 1927, feet
8	B-25-94-TX/T94-025	1994	900	5-85	Poor-Fair	20×12.5	NAD27 Texas State Planes, South Central Zone, US Foot
9	B-32-91-TX/T91-032	1991	2100	5-100	Poor	20×25	15N NAD 1927, feet
10	B-15a-89-TX/T89-15a	1989	850	5-80	Poor-Fair	61×61	NAD27 Texas State Planes, Southern Zone, US Foot
11	B-02-96-TX/T96-002	1996	650	5-80	Fair	20×12.5	15N NAD 1927, feet
12	B-32-97-TX/T97-032	1997	800	5-90	Fair	20×12.5	15N NAD 1927, feet
13	B-15-89-TX/T89-015	1989	800	10-65	Poor	30.5×305	15N NAD 1927, feet
14	B-43-91-TX/T91-043	1991	900	5-90	Fair	40×12.5	15N NAD 1927, feet

Table 2: The 3D seismic surveys uploaded for initial data quality analyses within Project Area 2.1. Projected coordinate systems: NAD_1927_BLM_Zone_15N [EPSG,32066], NAD27 Texas State Planes, Southern Zone and South-Central Zone [EPSG, 502270, 502089].

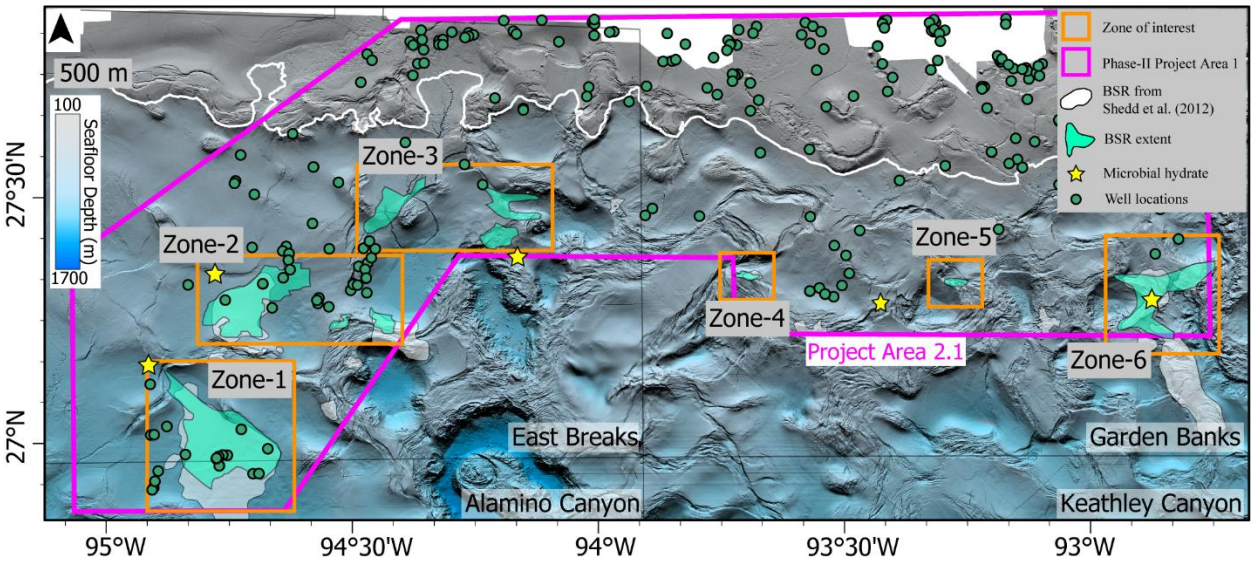

Figure 2: The bathymetry of Project Area 2.1 from Kramer and Shedd (2017)*. The white shapes represent the BSRs previously interpreted by BOEM (Shedd et al., 2012). Light green shapes represent the BSRs interpreted in this report. Interpreted BSRs are grouped into six zones shown by the orange rectangles. The white line shows the 500 m water depth contour. Yellow stars show the locations of piston cores where microbial hydrates were observed by Sassen et al (2001).*

2 RMS Mapping

To identify possible BSRs in Project Area 2.1, regional root-mean-square (RMS) amplitude calculations were performed independently within all 3D seismic surveys (Figure 1a). The detailed workflow can be found in the report for Phase 1 Project Area 1. However, the time windows vary in this report to show the clear extent of the BSRs. The time windows are kept larger in zones where BSR depths significantly vary.

Because of multiple heat-conductive shallow salt bodies in this area, the geothermal gradient is highly variable, which significantly perturbs the base of the gas hydrate stability zone. Therefore, RMS amplitude maps are computed within the different depth windows below the seafloor. RMS amplitude maps that correlate with the identified BSR zones are shown in Section 4 of this report.

3 Classification of BSRs

We classify BSRs into three different types based on their characteristics in the seismic data: continuous BSRs, discontinuous BSRs, and clustered BSRs. Continuous BSRs are continuous, coherent seismic reflections with reversed (trough-leading) polarity that crosscuts primary stratigraphy (Hillman et al., 2017; Vanneste et al., 2001). Discontinuous BSRs, also referred to as 'patchy BSRs', are characterized by segmented and non-coherent lateral reflections that typically align with the seafloor topography (Hillman et al., 2017; Shedd et al., 2012). A third type of BSR is called a clustered BSR, which is characterized as thick clustered assemblages of high amplitude reflections with its top roughly aligning with the overlying seafloor bathymetry (Portnov et al., 2019). In particular, clustered BSRs occur in the regions with folding or salt tectonics because these regions host multiple anticlinal and domal structures that can trap gas underneath the GHSZ. Such BSRs are common in the Gulf of Mexico and warrant special attention because these BSRs may indicate high concentrations of gas hydrate in turbidite sands (Portnov et al., 2019).

4 Results in Project Area 2.1

4.1 Zone 1

Zone 1 is located within the Diana Basin in the western part of Project Area 2.1 (Figure 2). The water depth in this zone ranges from 1200 to 1700 m. Within Zone 1, a single BSR system is observed. This BSR is the largest one identified in Project Area 2.1, covering an approximate area of 250 km^2 (Figure 3). This BSR was first described by Frye and others (2010) and was also identified by Shedd and others (2012). The extent of the BSR is smaller in this study as compared to previous interpretations possibly because BOEM used a proprietary data set with different acquisition and processing parameters than the publicly available dataset used in this study. The seismic data south of Zone 1 has not been released to the public. Herein, the BSR was mapped using the seismic volume B-43-91-TX and occurs at 250-600 milliseconds two-way travel time (TWT) below the seafloor (Figures 4-7). This depth corresponds to approximately 200-500 m below seafloor (mbsf), using an average sedimentary velocity of 1700 m/s.

Many wells are drilled in Zone 1, and from those, we have selected four specific wells as illustrated in Figure 3. Among these wells, the well log associated with API # 608044023300 exhibits a notable correlation with the seismic profile labeled as 'c-d' in Figure 5. At an approximate TWT of 2470 msec, which corresponds to a depth of 6230 ft below sea level, the BSR intersects with the well. Despite the absence of any observed lithological changes in the gamma ray log, there is a discernible increase in resistivity from 5880 to 6410 ft true vertical depth (TVD). This increase in resistivity surpasses the background resistivity (~1 Ωm) by 1 to 6 Ωm. This suggests that hydrates might be present near this particular well, albeit in low concentrations.

Frye and others (2010) observed an extensive deepwater fan system in this area, which may be a potential reservoir for gas hydrate (Figure 3). The fan is visible on seismic cross sections with high amplitude peak and trough leading reflections in seismic data (Figure 6). These high reflectivity zones associated with the fan system span an area of 35 km^2 (Figure 3). JIP Leg 2 Holes AC21-A and AC 21-B along with the well API # 608044016000 are drilled into these peak anomalies (Frye et al., 2010). Figures 7 and 8 show the seismic data associated with the wells. Low gamma ray and modest increases in resistivity are observed in these wells (Figure9) within the interval that intersects with these peak leading reflections (Cook and Tost, 2014; Frye et al., 2010). The low gamma ray and poor sediment cohesion (as inferred by the increase in borehole size, Figure 9) suggests that these intervals are sand dominated (Frye et al., 2010). Frye et al. (2010) interpreted these sand intervals as hosting hydrate with low to moderate saturations (20% to 40%). Cook and Tost (2014) interpreted these logs differently and suggested that observed modest increase in resistivity within these intervals was caused by water saturated low porosity sand.

Figure 9 is a cross section across four wells, AC21-A, AC21-B, 608044023300, 608044016000, that shows the sand interval and the depth of the BSR or the base of hydrate stability; the orientation of this cross section is shown in Figure 3. In addition, we also add Horizon H1 (Figures 4-8) as a reference layer on the cross section (Figure 9), because H1 a prominent shallow horizon in this region that intersects all four wells. AC21-A, B and well with API #608044016000 show a clear decrease in gamma rays within H1, indicating a sand rich layer interval. This signature is not observed in borehole with API # 608044023300. Because AC21- A, B wells are outside the identified BSR zone, estimated depth is shown in these wells (Figure 9).

We derive geothermal gradients from the BSR assuming an equilibrium model: 1) heat flow is constant, one-dimensional (vertical) and occurs only through conduction; 2) pore pressure is hydrostatic; 3) pore fluid salinity is 3.5 %; and 4) gas composition is pure methane. We estimate the geothermal gradient in Zone-1 between 30°- 55° C/km (Table 3). The average geothermal gradient is around ~30° C/km, but near the salt, especially in the northwestern part, geothermal gradient increases up to 55° C/km.

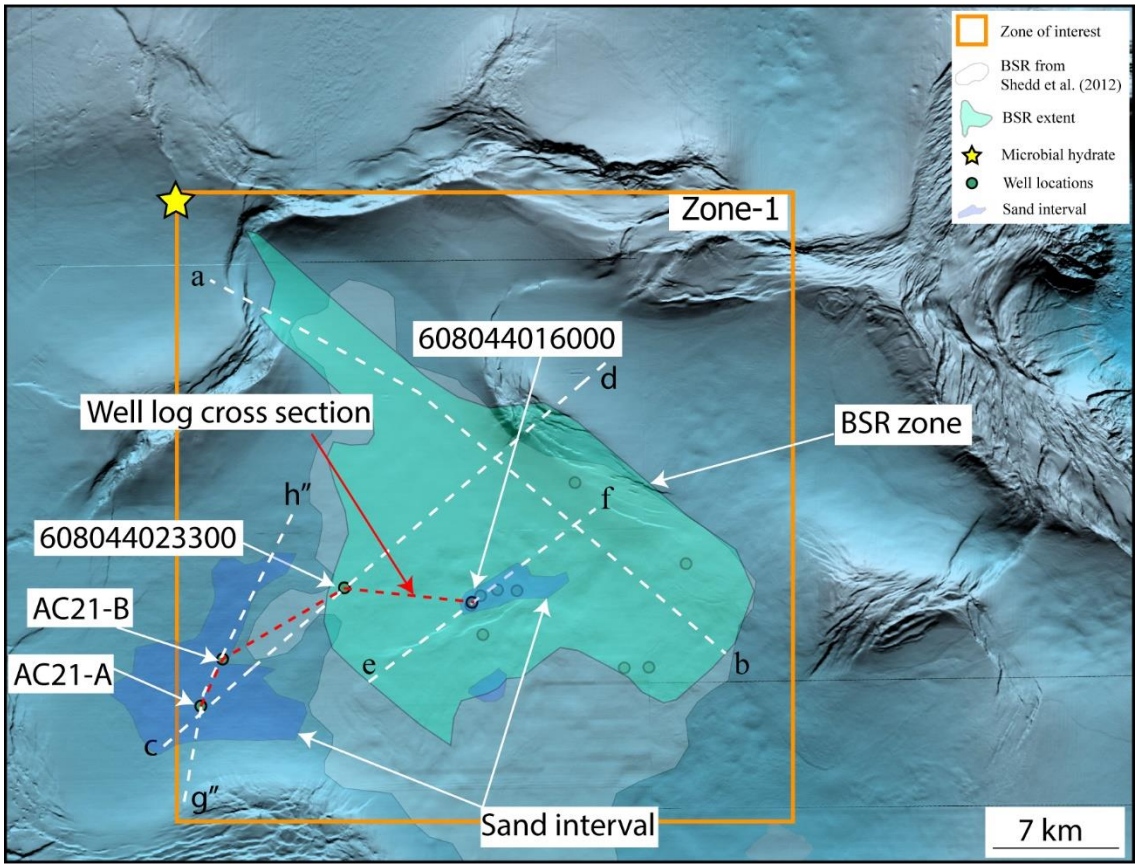

Figure 3: A bathymetry map showing a BSR extent within Zone-1 of Project Area 2.1 (Kramer and Shedd, 2017). *The map also highlights sand intervals, in part interpreted from the presence of an interval with high peak leading reflections followed by trough leading reflections in the seismic data. White dashed lines show the track of seismic profiles.*

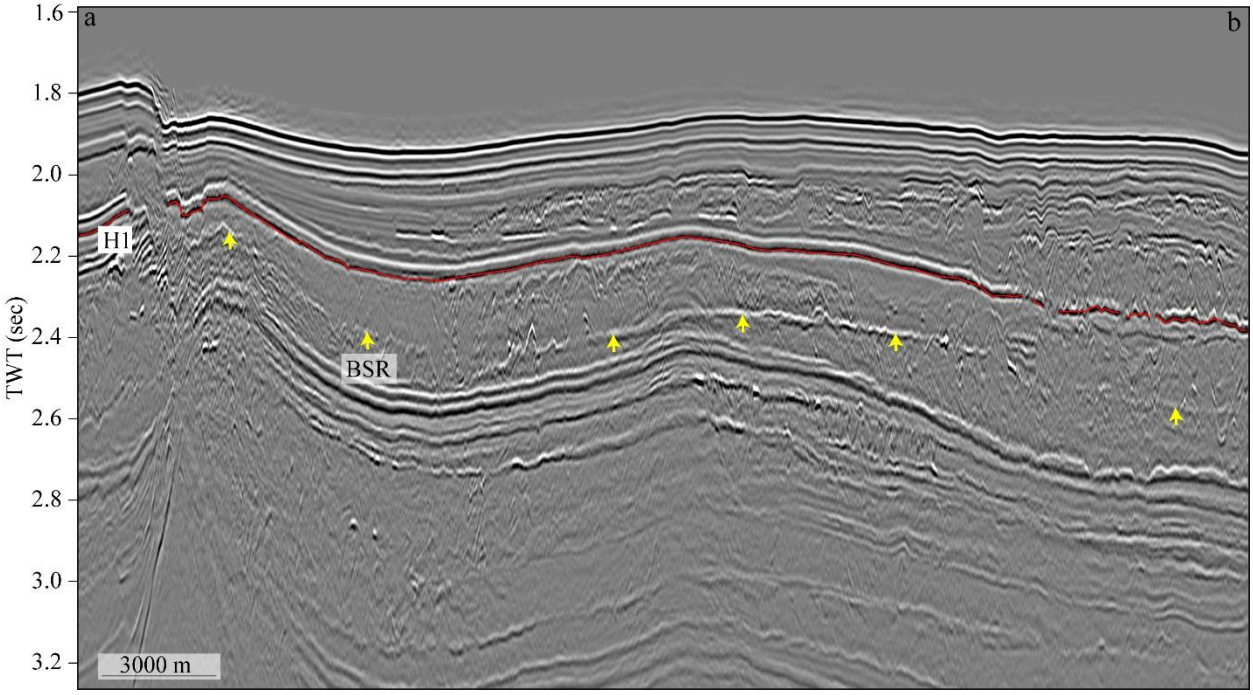

Figure 4: Seismic profile a-b showing a northwest-southeast cross-section across the BSR system of Zone-1. The BSR is shown by the yellow arrows. The profile location is shown in Figure 3.

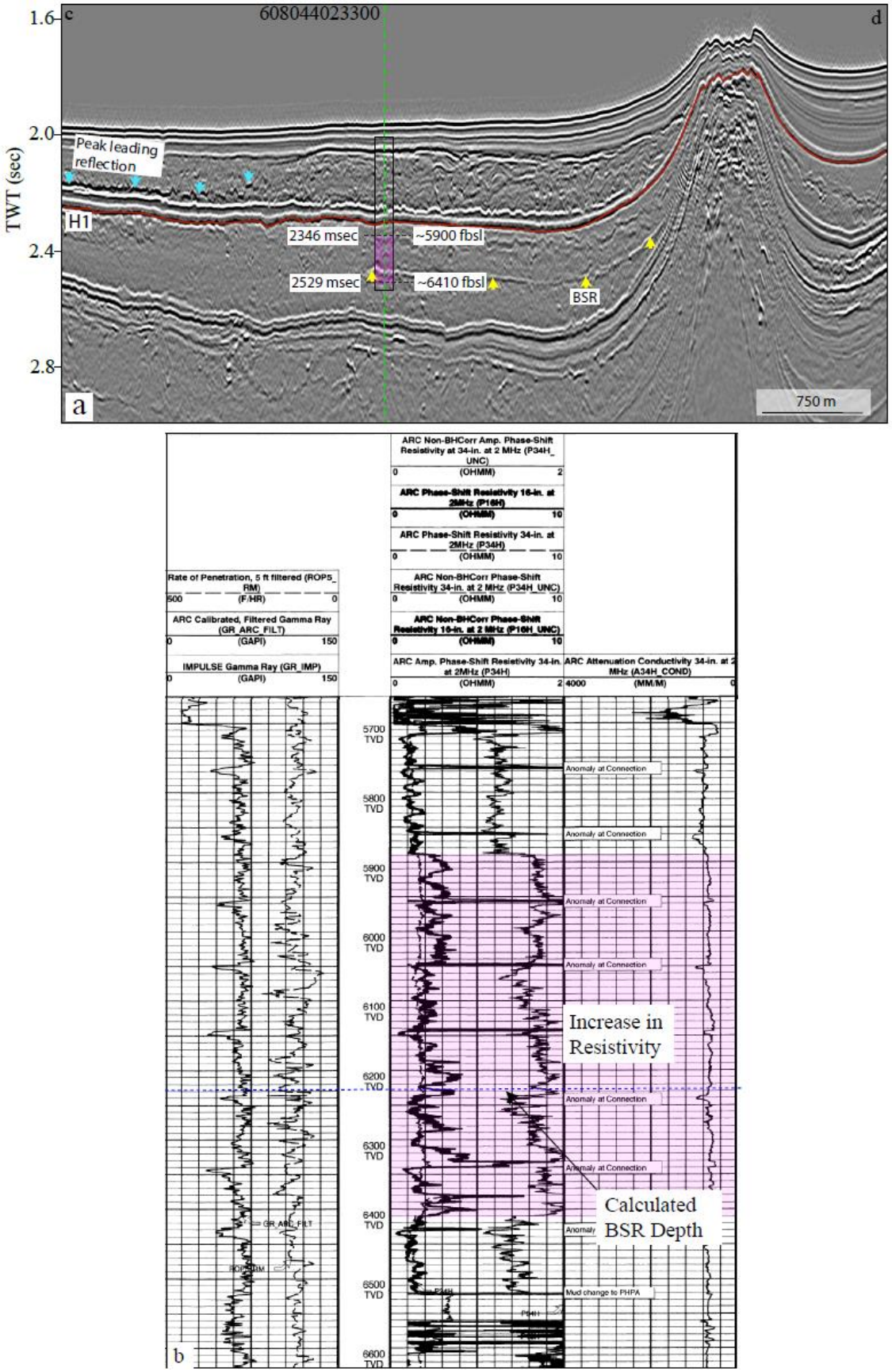
c
608044023300
d
1.6
2.0
2.4
2.8
TWT (sec)
Peak leading reflection
H1
2346 msec
~5900 fbsl
2529 msec
~6410 fbsl
BSR
a
750 m
ARC Non-BHCorr Amp. Phase-Shift Resistivity at 34-in. at 2 MHz (P34H_UNC)
ARC Phase-Shift Resistivity 16-in. at 2MHz (P16H)
ARC Phase-Shift Resistivity 34-in. at 2MHz (P34H)
ARC Non-BHCorr Phase-Shift Resistivity 34-in. at 2 MHz (P34H_UNC)
ARC Non-BHCorr Phase-Shift Resistivity 16-in. at 2 MHz (P16H_UNC)
Rate of Penetration, 5 ft filtered (ROP5_RM)
ARC Calibrated, Filtered Gamma Ray (GR_ARC_FILT)
IMPULSE Gamma Ray (GR_IMP)
ARC Amp. Phase-Shift Resistivity 34-in. at 2MHz (P34H)
ARC Attenuation Conductivity 34-in. at 2 MHz (A34H_COND)
5700 TVD
5800 TVD
5900 TVD
6000 TVD
6100 TVD
6200 TVD
6300 TVD
6400 TVD
6500 TVD
6600 TVD
Anomaly at Connection
Increase in Resistivity
Calculated BSR Depth
Mud change to PHPA
b

Figure 5: a) Seismic profile c-d showing a southwest-northeast cross-section across the BSR system of Zone-1. The BSR is shown by the yellow arrows. The green line shows the well location on the seismic profile and corresponding well logs are shown in Figure b). The interval with a slight increase in resistivity is highlighted in light purple color. This moderate increase in resistivity is likely attributed to the presence of hydrate in low saturation. The seismic profile location is shown in Figure 3.

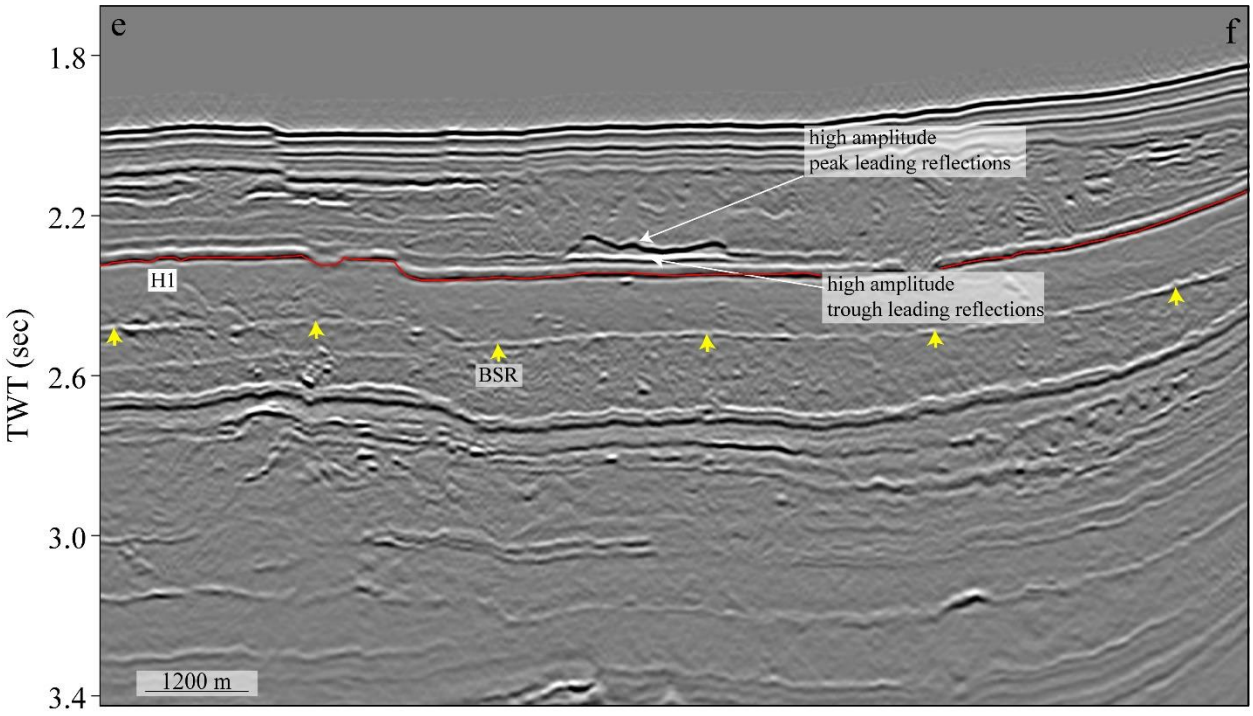

Figure 6: Seismic profile e-f showing a southwest-northeast cross-section across the BSR system of Zone-1. The BSR is shown by the yellow arrows. The high peak leading amplitude and the associated trough is part of the deepwater fan system in the area. The profile location is shown in Figure 3.

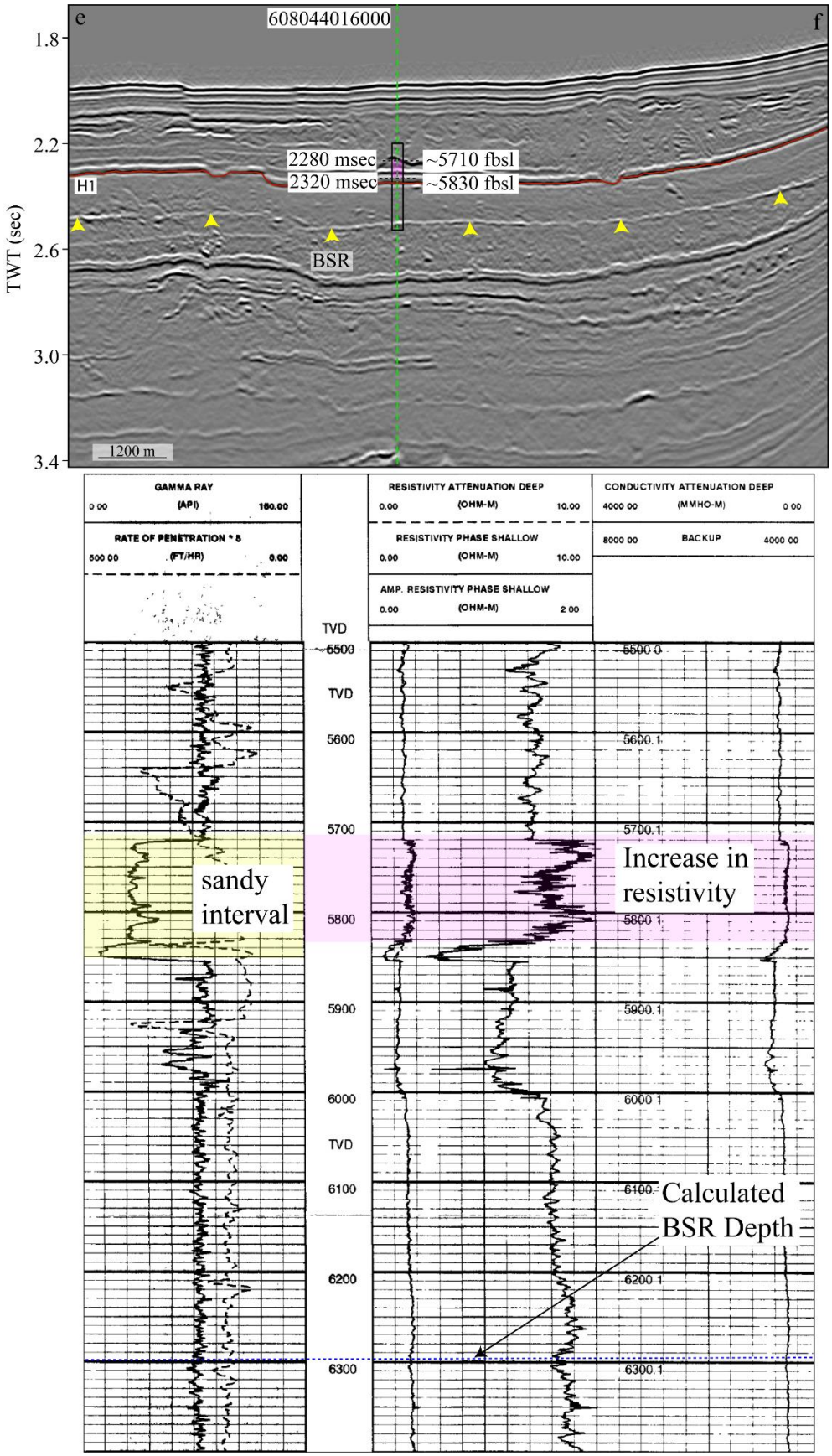
e
608044016000
f
1.8
2.2
2.6
3.0
3.4
TWT (sec)
2280 msec
~5710 fbsl
2320 msec
~5830 fbsl
H1
BSR
1200 m
GAMMA RAY
0.00 (API) 150.00
RATE OF PENETRATION * 5
500.00 (FT/HR) 0.00
RESISTIVITY ATTENUATION DEEP
0.00 (OHM-M) 10.00
RESISTIVITY PHASE SHALLOW
0.00 (OHM-M) 10.00
AMP. RESISTIVITY PHASE SHALLOW
0.00 (OHM-M) 2.00
CONDUCTIVITY ATTENUATION DEEP
4000.00 (MMHO-M) 0.00
8000.00 BACKUP 4000.00
TVD
6500
5500.0
5600
5600.1
5700
5700.1
5800
5800.1
5900
5900.1
6000
6000.1
6100
6100.1
6200
6200.1
6300
6300.1
sandy interval
Increase in resistivity
Calculated BSR Depth

Figure 7: a) Seismic profile e-f showing a southwest-northeast cross-section across the BSR system of Zone-1. The BSR is shown by the yellow arrows. The green line shows the well location on the seismic profile and corresponding well logs are shown in Figure b). The interval of interest is highlighted in yellow to indicate the sand and light purple color which indicates higher resistivity. A low gamma ray value suggests a sandy interval, while a slight increase in resistivity could be attributed to either low saturation hydrate or a lithological variation. Interval of interest is also highlighted on the seismic section. The seismic profile location is shown in Figure 3.

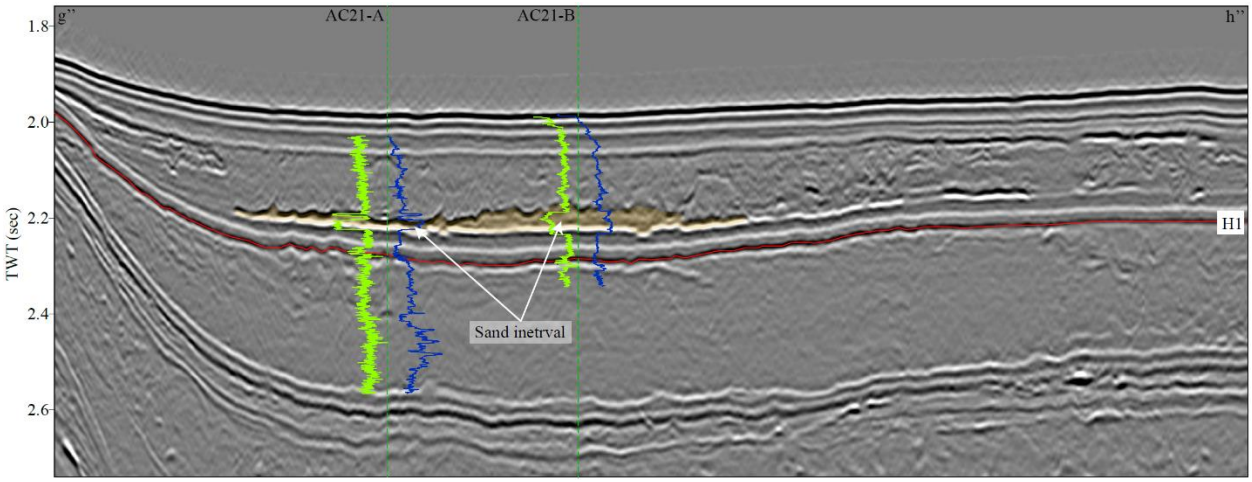

Figure 8: Seismic profile g''-h'' across the sand interval of Zone-1. The profile location is shown in Figure 3. The gamma ray (green) and resistivity (blue) logs from wells AC21-A and AC21-B are projected on the seismic section. To see the scales of these logs please see Figures 9 and 10.

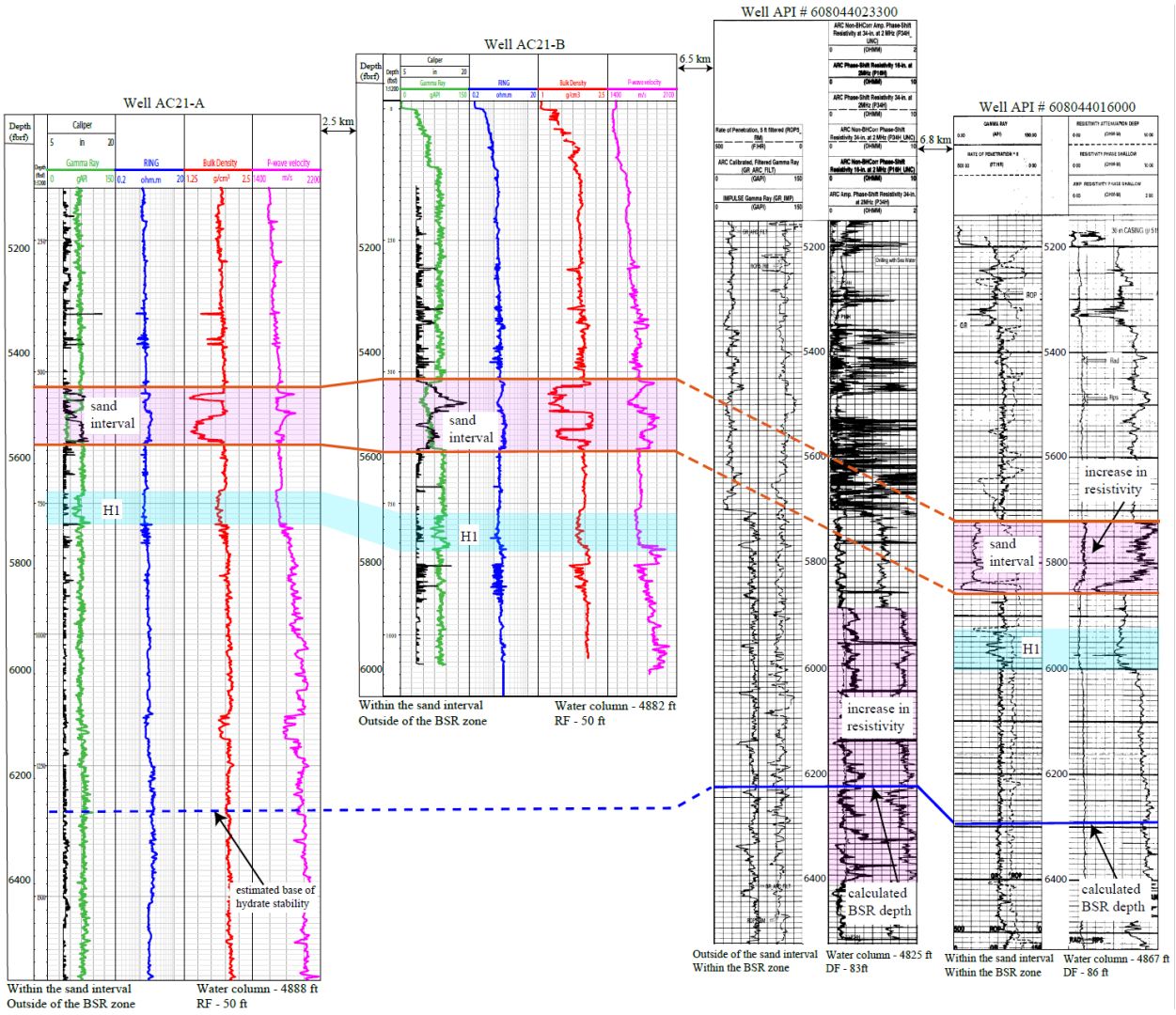

Figure 9: A cross section across four wells showing the correlation of the sand interval, Horizon H1, and the BSR depth (blue line) or the estimated base of gas hydrate stability (blue dashed line). The sand interval is highlighted in pink and horizon H1 is highlighted in light blue. The cross section track is shown with a red dotted line on Figure 3.

Zone	Seafloor TWT (msec)	BSR TWT (msec)	Seafloor Depth (m)	BSR Depth (mbsf)	BSR depth (mbss)	Geothermal Gradient (°C/km)
1	1600 - 2270	2000 - 2600	1200 - 1700	200 - 500	1600-2000	30 - 55
2	1200 - 1800	1430 - 2100	900 - 1350	110 - 300	1150-1650	35 - 75
3	870 - 1870	1300 - 1850	650 - 1400	100 - 400	1050 -1475	25 - 65
4	1130 - 1330	1300 - 1400	850 - 1000	140 - 270	1050 -1200	30 - 40
5	930 - 1600	1100 - 1800	700 - 1200	75 - 475	900 - 1400	20 - 65
6	1000 - 1730	1100 - 2000	750 - 1300	170 - 450	1050-1450	20 - 55

Table 3: The seafloor depth, BSRs depth and geothermal gradient in the identified zones.

4.2 Zone 2

Zone 2 is located within the East Breaks protraction area (Figure 2). The water depth in this zone varies from 900 to 1350 m. We have identified and mapped three distinct BSR systems within Zone 2 (Figure 10). All three BSR systems were previously identified by BOEM.

The largest BSR system in Zone 2 covers an approximate area of 170 km^2, while the BSRs in the middle and eastern parts encompass 9 and 17 km^2, respectively. The depths of the BSRs in this zone range from 130 msec TWT (~110 mbsf) to 310 msec TWT (~260 mbsf) below the seafloor. Figures 11-17 display the BSRs across these BSR zones. Although various types of BSRs are observed in Zone 2, most of them are discontinuous, which may suggest interbedded layers with alternating or intermittent course-grained layers containing gas hydrate and/or gas. In certain locations, BSRs are found within highly faulted settings, as depicted in Figure 12. In the north-south seismic profile (profile i-j) across the largest BSR in Zone 2, clustered BSRs are observed (Figure 11). The extent of these clustered BSRs is illustrated in Figure 10, covering an area of approximately 19 km^2 when combined.

Within Zone 2, there are several wells that penetrate the mapped BSR. One such well (API # 608044018600), is located within the mapped clustered BSR area (Figure 10), and the log data are displayed in Figure 11. In this particular well, we observe a very small increase in resistivity (less than 0.5 Ωm) between 4520 and 5990 ft. This interval correlates to the clustered BSR and related high amplitude reflections below the BSR (Figure 11). Although the increase in resistivity is not substantial (less than 0.5 Ωm), it may suggest the presence of hydrates or gas in low concentrations.

Other wells in this zone, which are not shown in this report, either lack shallow data or do not exhibit any variations in resistivity within the hydrate stability zone or at and below the BSR.

In seismic profile i-j shown in Figure 11, the BSR is very shallow above the salt at the southern side, as shallow as 110 m below the seafloor. The estimated geothermal gradient is nearly 75°C/km. Further away from the salt, the geothermal gradient reduces and averages 35 °C/km.

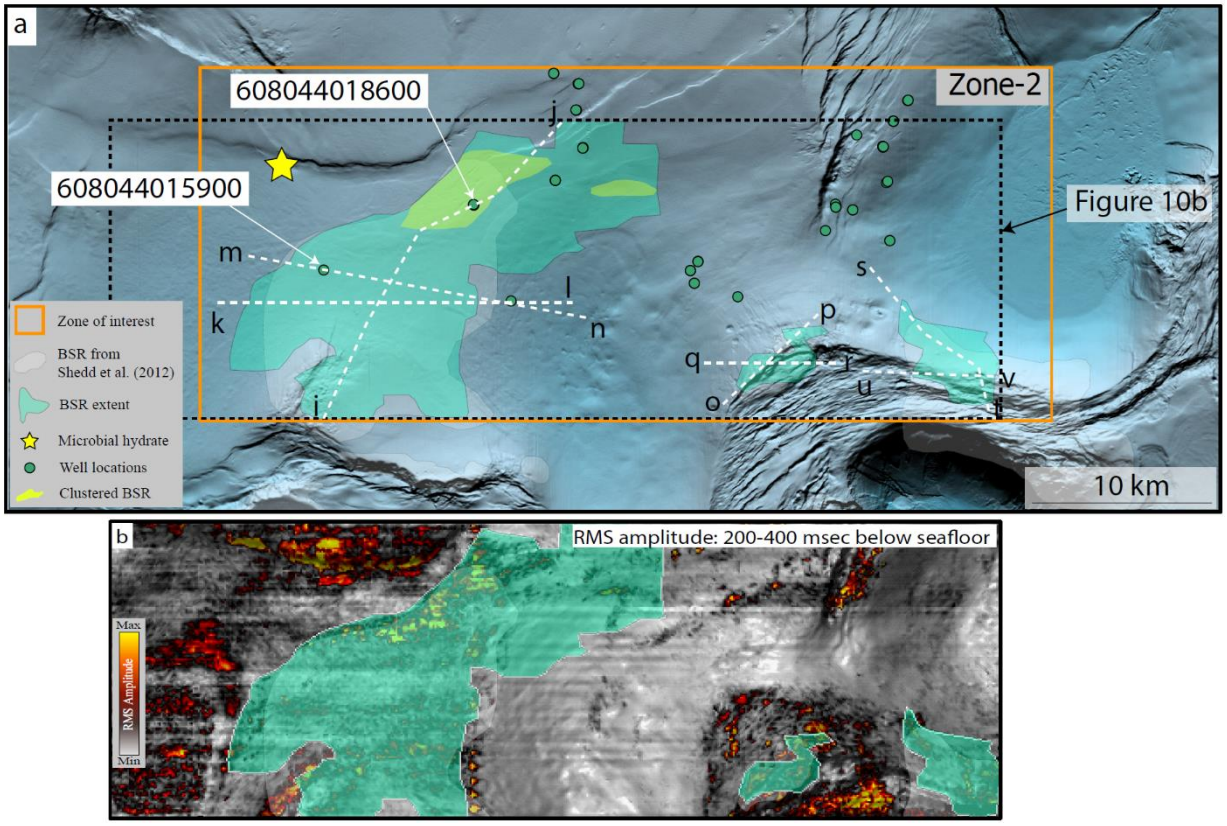

Figure 10: a) A bathymetry map showing the BSR extent within Zone-2 of Project Area 2.1 (Kramer and Shedd, 2017). White dashed lines show the track of seismic profiles. b) An RMS amplitude map of the dashed area in Figure 10a with a 200 - 400 msec window below the seafloor. Some of the high amplitudes correlate to the mapped BSR zones. The RMS amplitude map is generated using the seismic volume B-15-89-TX.

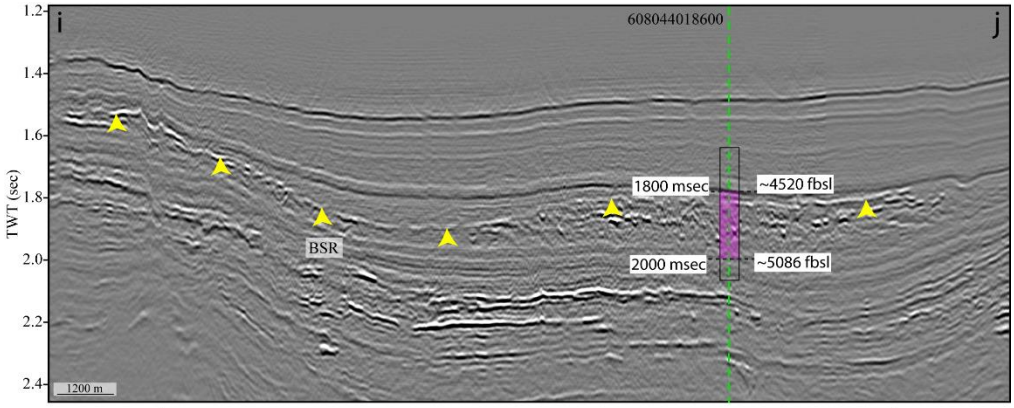
i
j
608044018600
TWT (sec)
1.2
1.4
1.6
1.8
2.0
2.2
2.4
BSR
1800 msec
2000 msec
~4520 fbsl
~5086 fbsl
1200 m

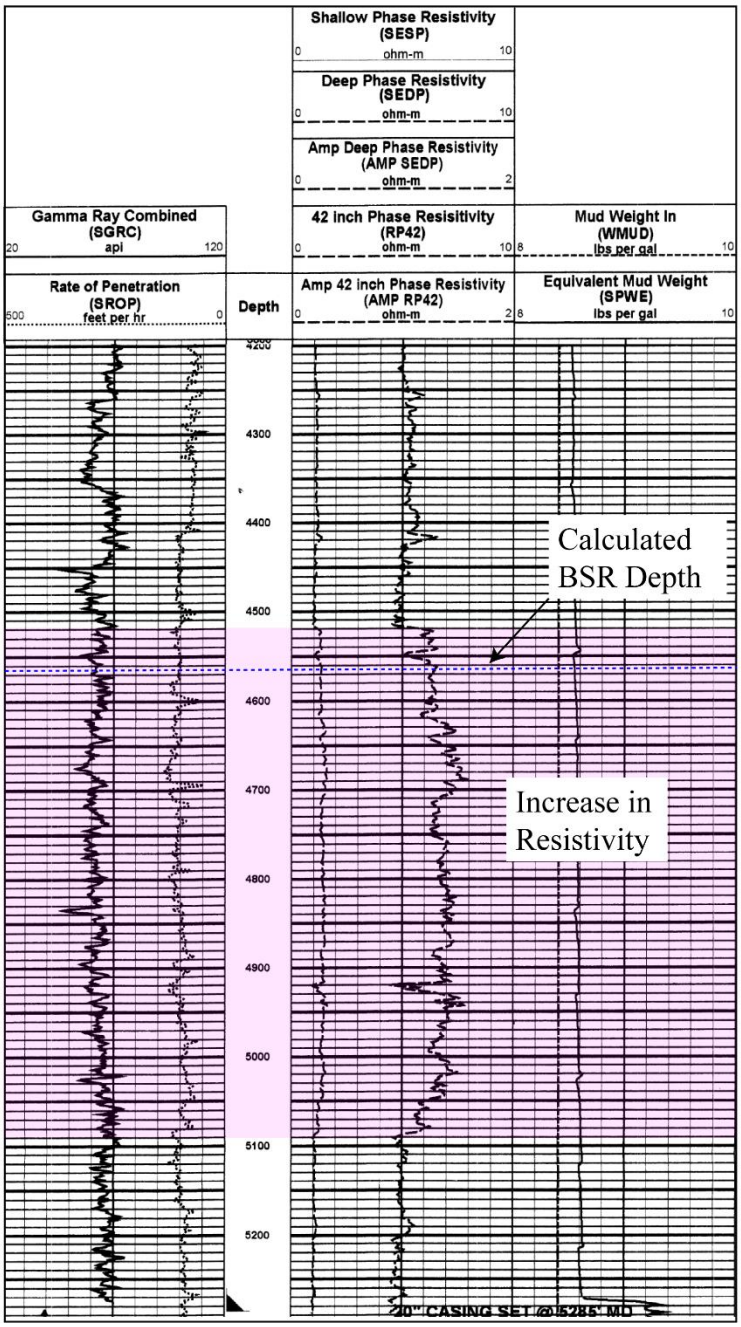
Shallow Phase Resistivity (SESP)
0 ohm-m 10
Deep Phase Resistivity (SEDP)
0 ohm-m 10
Amp Deep Phase Resistivity (AMP SEDP)
0 ohm-m 2
Gamma Ray Combined (SGRC)
20 api 120
42 inch Phase Resistivity (RP42)
0 ohm-m 10
Mud Weight In (WMUD)
8 lbs per gal 10
Rate of Penetration (SROP)
500 feet per hr 0
Depth
Amp 42 inch Phase Resistivity (AMP RP42)
0 ohm-m 2
Equivalent Mud Weight (SPWE)
8 lbs per gal 10
4200
4300
4400
4500
4600
4700
4800
4900
5000
5100
5200
Calculated BSR Depth
Increase in Resistivity
20" CASING SET @ 5285' MD

Figure 11: a) Seismic profile i-j showing a southwest-northeast cross-section across the largest BSR system of Zone-2. The BSR is shown by the yellow arrows. The green line shows the well location on the seismic profile and corresponding well logs are shown in Figure b). The resistivity on the profile shows only a very slight increase, which may suggest a very low saturation of hydrate above the BSR and very low free gas below it. It should be clearly noted, however, that this low variation in resistivity could also be due to a reduction in porosity. The seismic profile location is shown in Figure 10a.

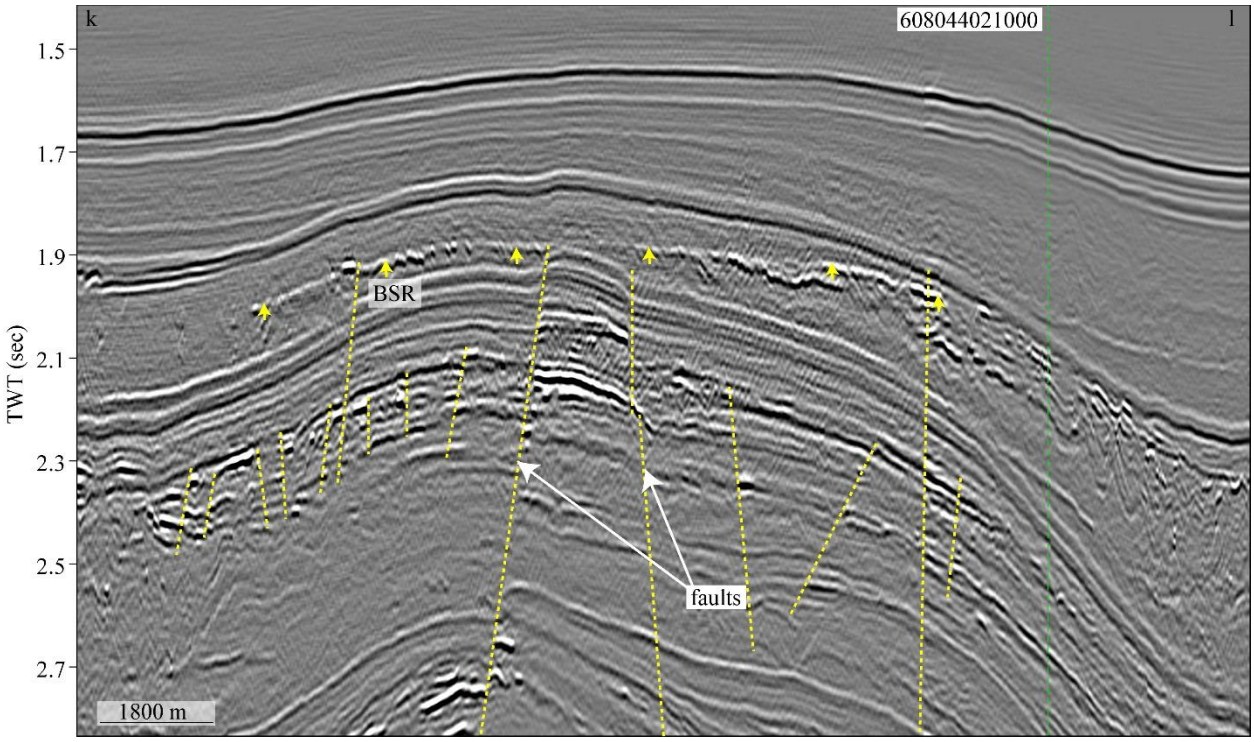

Figure 12: Seismic profile k-l showing a west-east cross-section across the largest BSR system of Zone-2. The BSR is shown by the yellow arrows. The profile location is shown in Figure 10a.

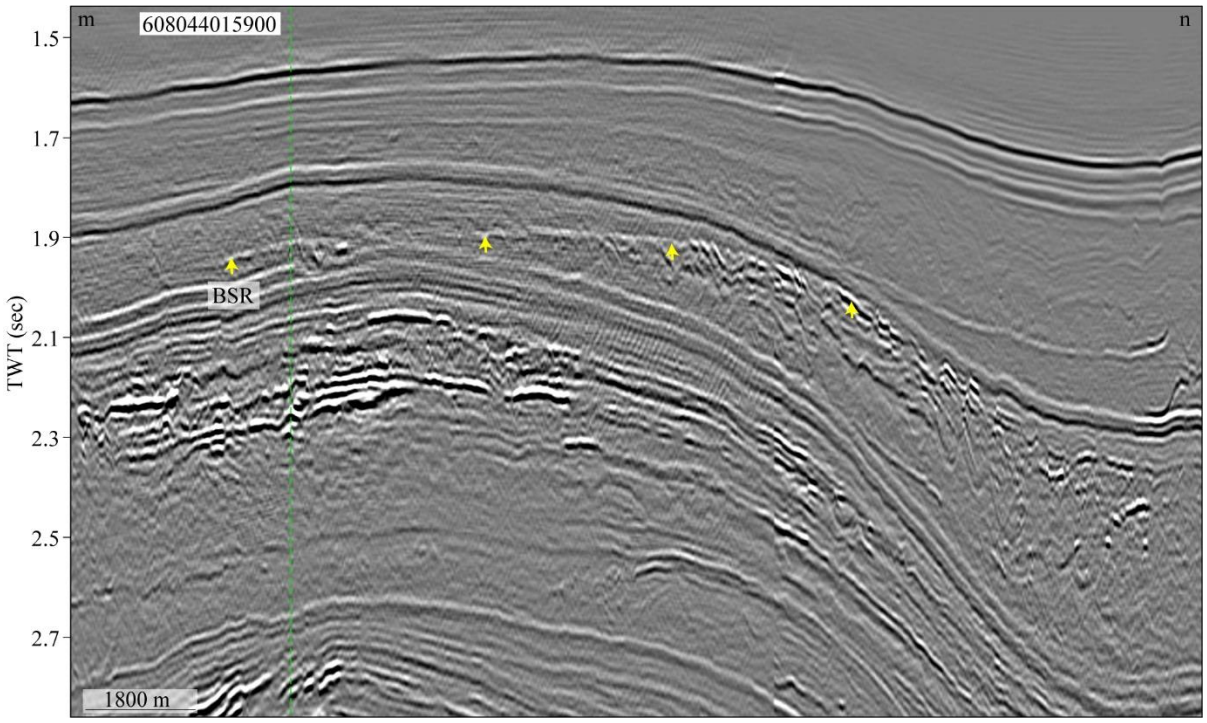

Figure 13: Seismic profile m-n showing a west-east cross-section across the largest BSR system of Zone-2. The BSR is shown by the yellow arrows. The profile location is shown in Figure 10a.

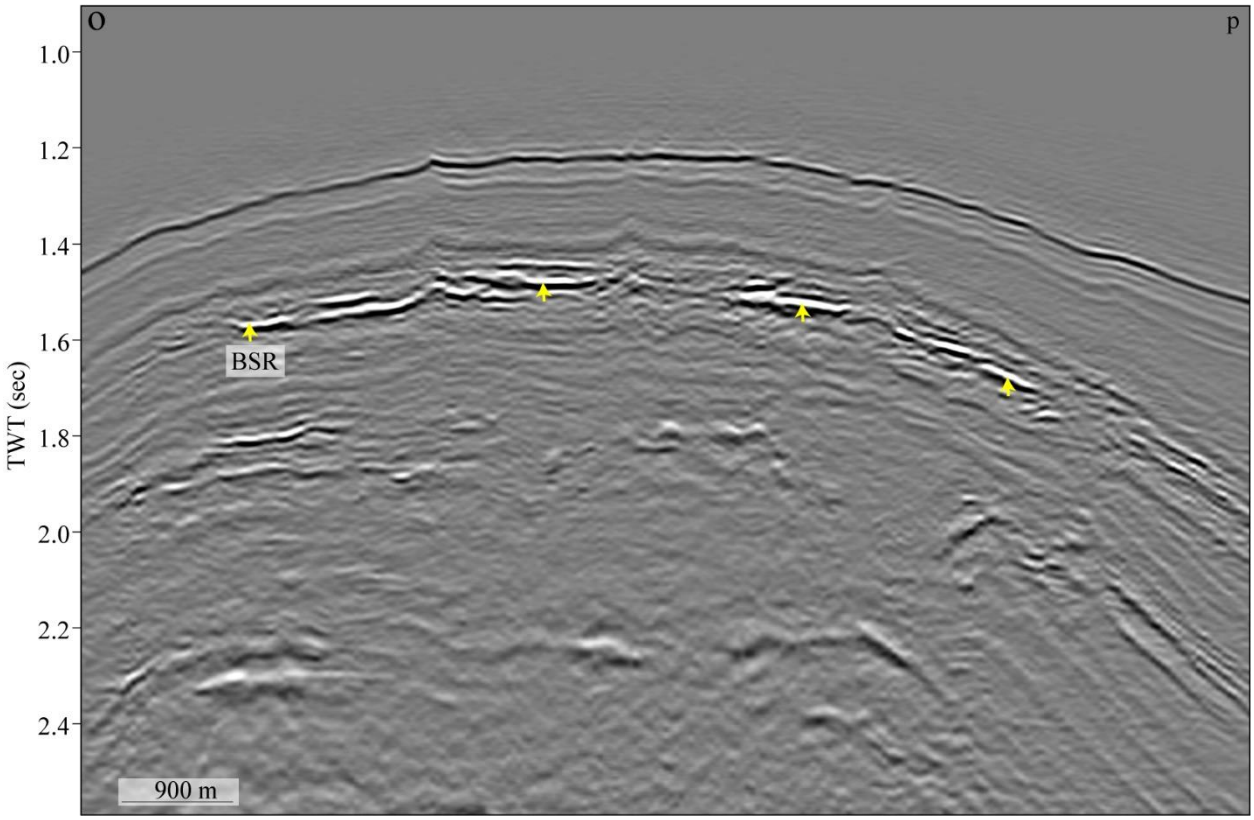

Figure 14: Seismic profile o-p showing a southwest-northeast cross-section across the central BSR system of Zone-2. The BSR is shown by the yellow arrows. The profile location is shown in Figure 10a.

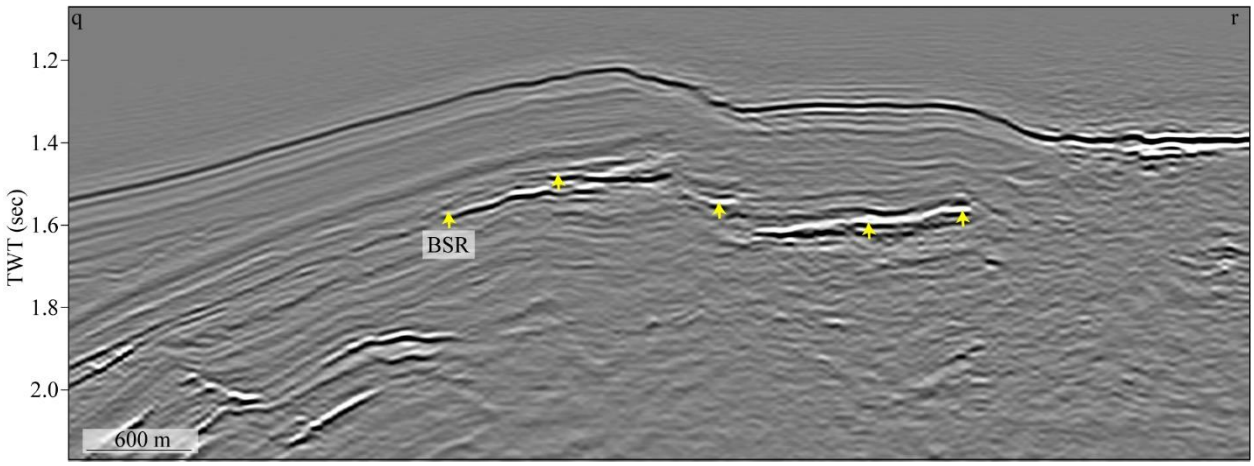

Figure 15: Seismic profile q-r showing a west-east cross-section across the central BSR system of Zone-2. The BSR is shown by the yellow arrows. The profile location is shown in Figure 10a.

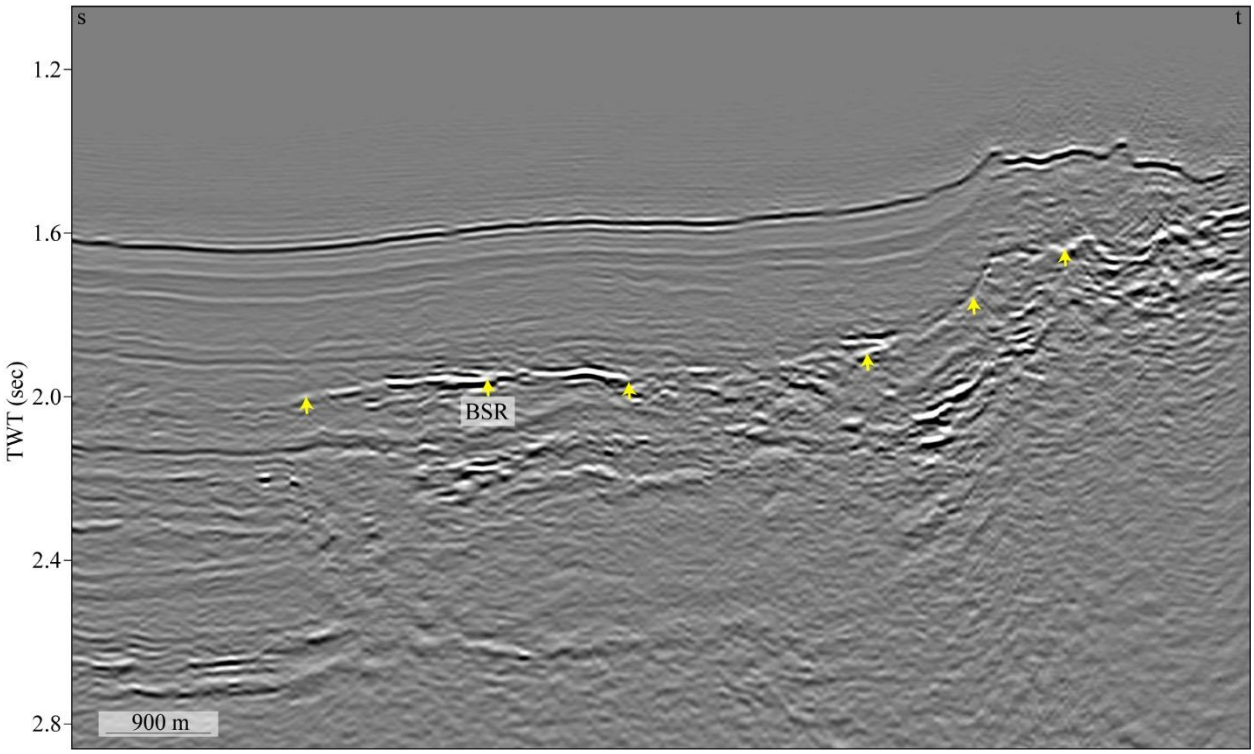

Figure 16: Seismic profile s-t showing a northwest-southeast cross-section across the eastern BSR system of Zone-2. The BSR is shown by the yellow arrows. The profile location is shown in Figure 10a.

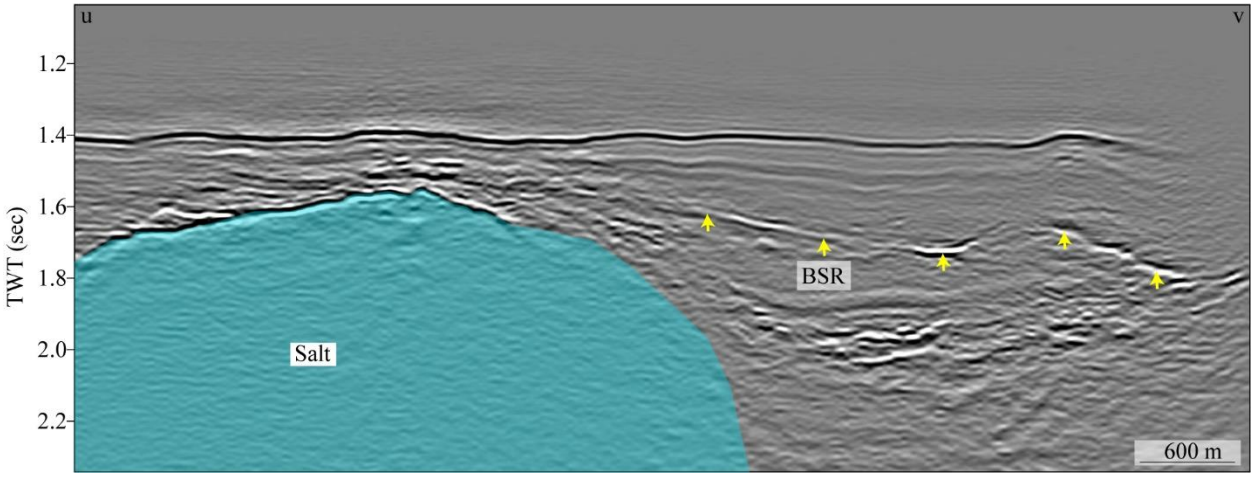

Figure 17: Seismic profile u-v showing a west-east cross-section across the eastern BSR system of Zone-2. The BSR is shown by the yellow arrows. The profile location is shown in Figure 10a.

4.3 Zone 3

Zone 3 is within the East Breaks protraction area, with water depths ranging from 650 m to 1400 m. In Zone 3, we have identified three BSR systems, none of which were previously mapped by BOEM (Figure 18). These BSRs are identified using the seismic volumes B-15a-89-TX and B-32-97-TX. The largest BSR system in Zone 3 is located on the western side and has an area of ~50 km^2. The BSR systems in the eastern and southeastern regions cover areas of around 40 km^2 and 28 km^2, respectively.

The BSR depths within this zone range from 120 msec to 450 msec TWT beneath the seafloor, corresponding to depths of ~100 m to ~400 m below the seafloor when assuming an average velocity of 1700 m/sec in the shallow sediments. The seismic profiles in Figures 19-24 depict the BSRs in Zone 3. Notably, a significant clustered BSR is observed within the southeastern BSR system (see Figures 21 and 22). This clustered BSR covers an area of approximately 14 km^2, as shown in Figure 18.

There are no wells in close proximity to the southeastern BSR system. Moreover, the wells closest to the eastern and western BSRs (refer to Figure 2) do not contain any well log data in the shallow interval.

Modern channels are clearly visible on the seafloor within Zone 3 of Project Area 2.1, as illustrated in Figure 18. Furthermore, paleochannels are visible in the subsurface on seismic data (Figure 19). However, due to limitations in the quality of the seismic data, the delineation of these paleochannels in map view is not possible.

The estimated geothermal gradient on the eastern BSR system is higher, reaching up to 65°C/km above the salt layer while the estimated geothermal gradient in the western BSR system where no shallow salt is present is approximately 25°C/km.

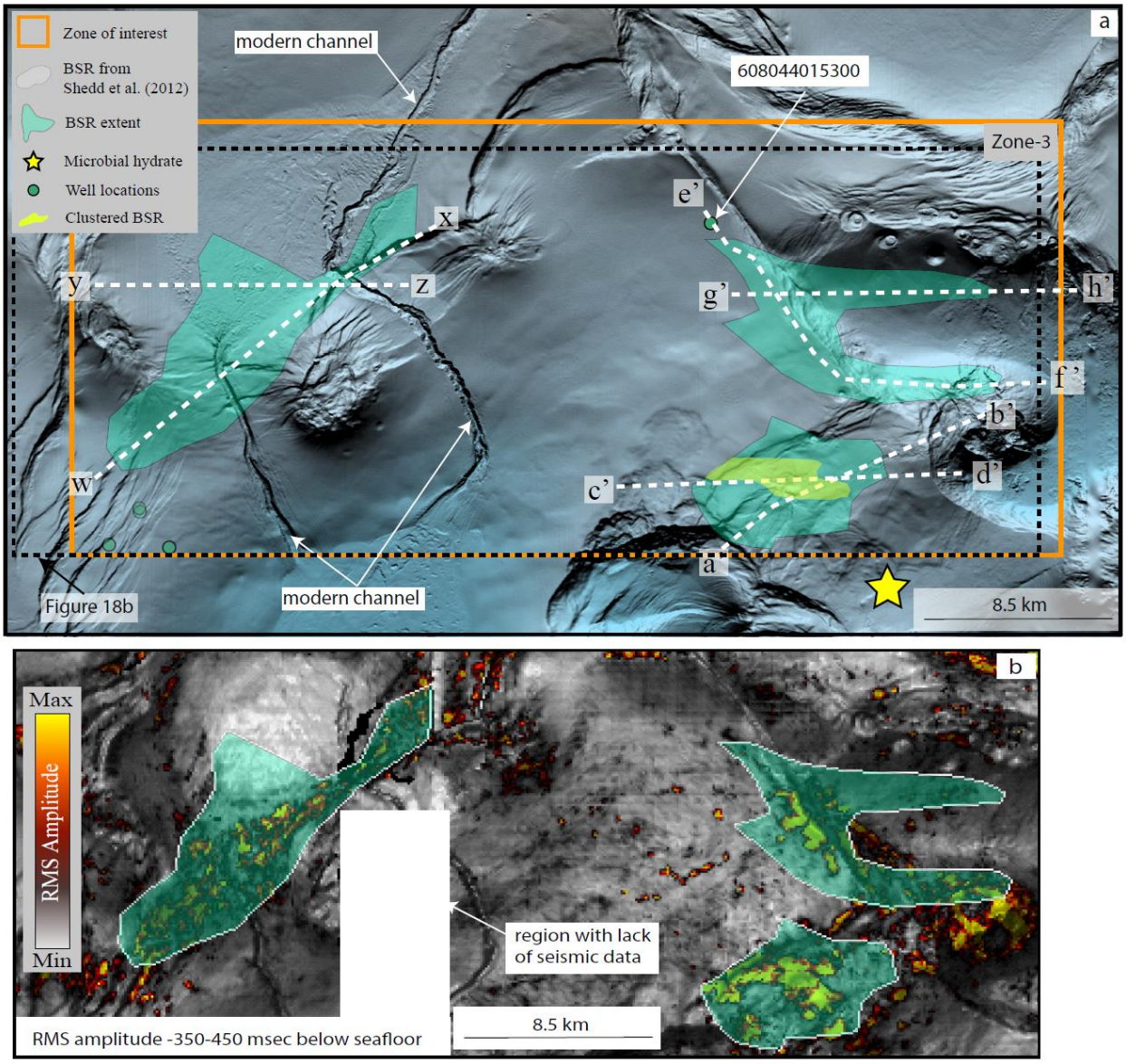

Figure 18: a) A bathymetry map showing the BSR extent within Zone-3 of Project Area 2.1 (Kramer and Shedd, 2017). White dashed lines show the track of seismic profiles. b) An RMS amplitude map within 350 - 450 msec window below the seafloor highlights areas with elevated amplitudes corresponding to the BSR zones. The RMS amplitude map is generated using the seismic volumes B-15a-89-TX and B-32-97-TX.

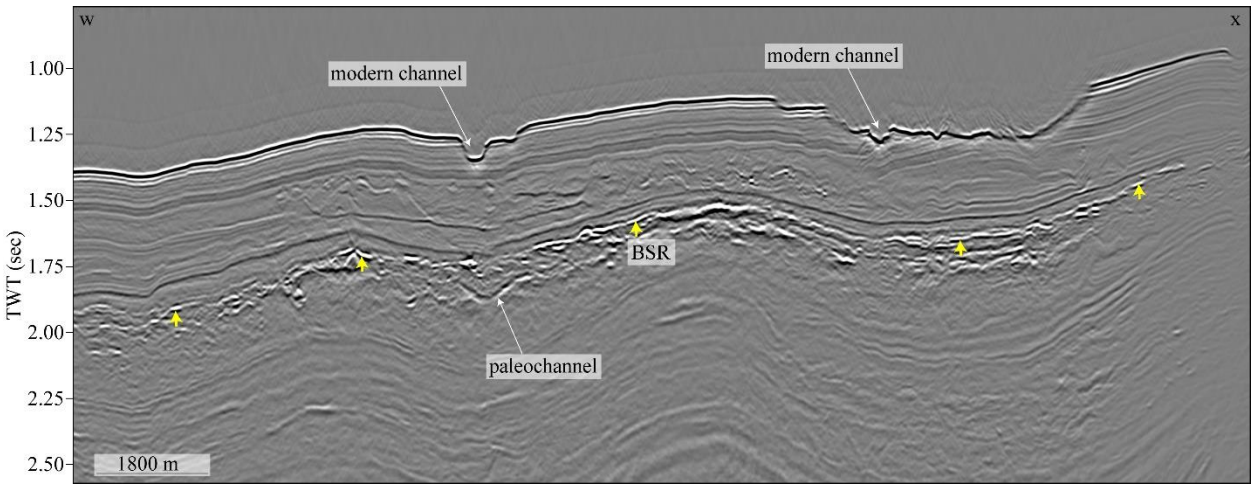

Figure 19: Seismic profile w-x showing a southwest-northeast cross-section across the western BSR system in Zone-3. The BSR is shown by the yellow arrows. The profile location is shown in Figure 18a.

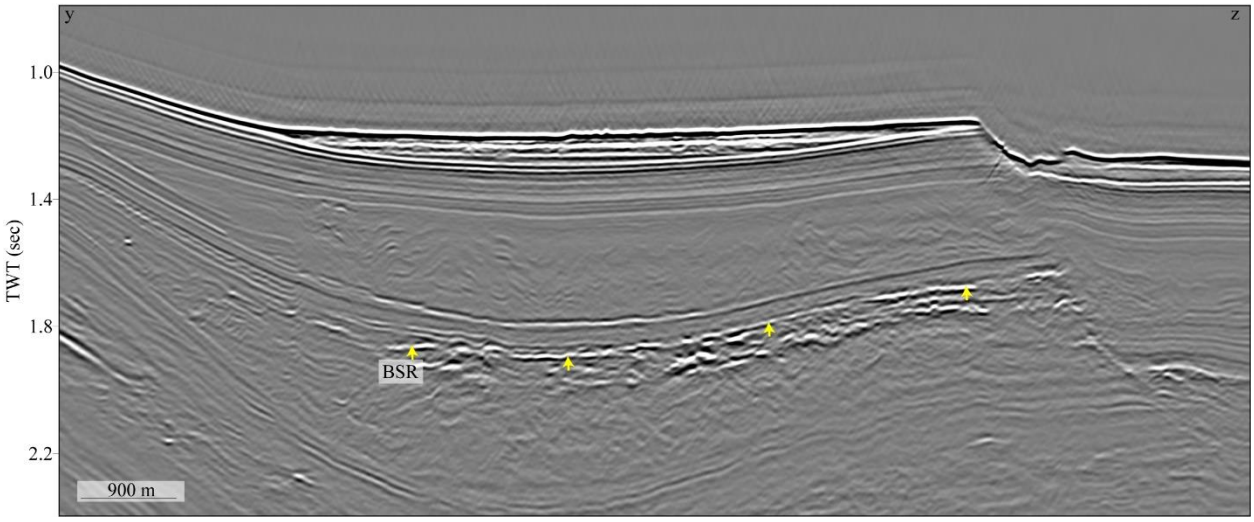

Figure 20: Seismic profile y-z showing a west-east cross-section across the western BSR system in Zone-3. The BSR is shown by the yellow arrows. The profile location is shown in Figure 18a.

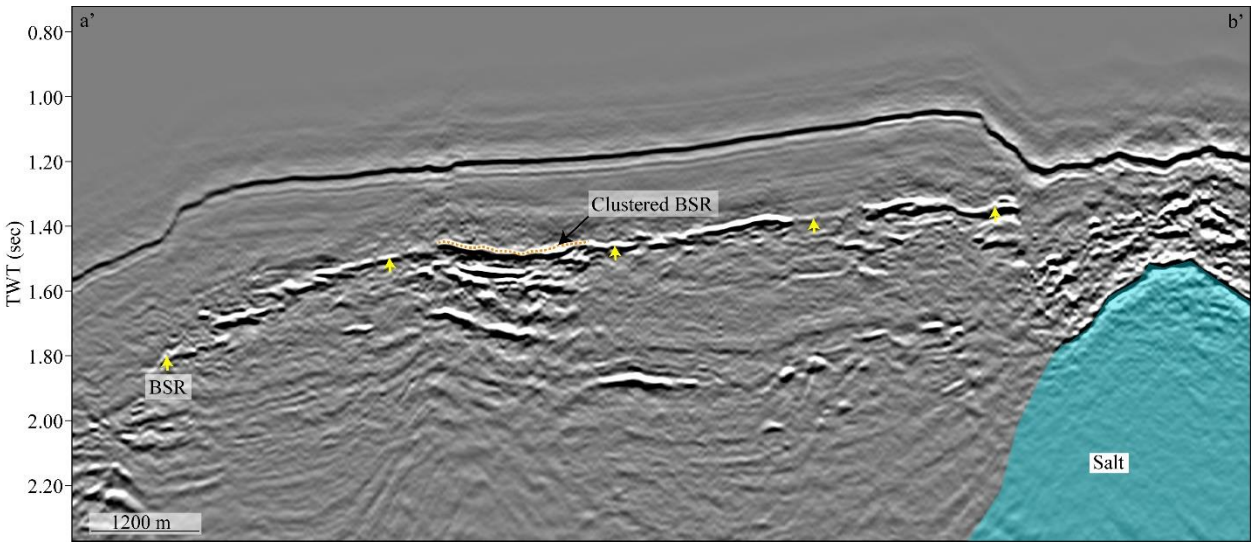

Figure 21: Seismic profile a'-b' showing a southwest-northeast cross-section across the southeastern BSR system of Zone-3. The yellow arrows indicate the location of the BSR, while the extent of the clustered BSR is represented by the dotted orange line. The profile location is shown in Figure 18a.

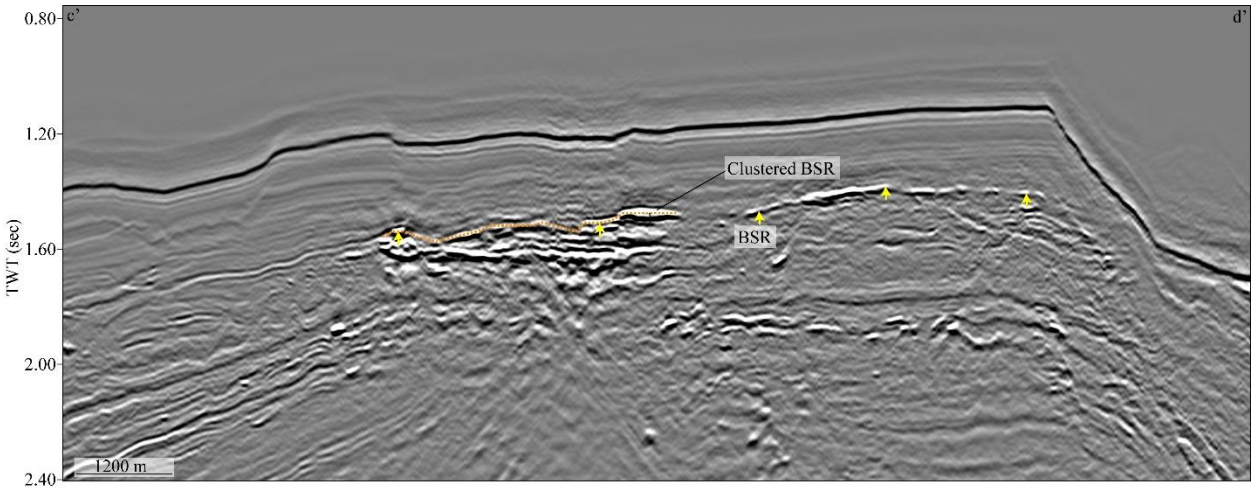

Figure 22: Seismic profile c'-d' showing a west-east cross-section across the southwestern BSR system of Zone-3. The BSR is shown by the yellow arrows. The profile location is shown in Figure 18a.

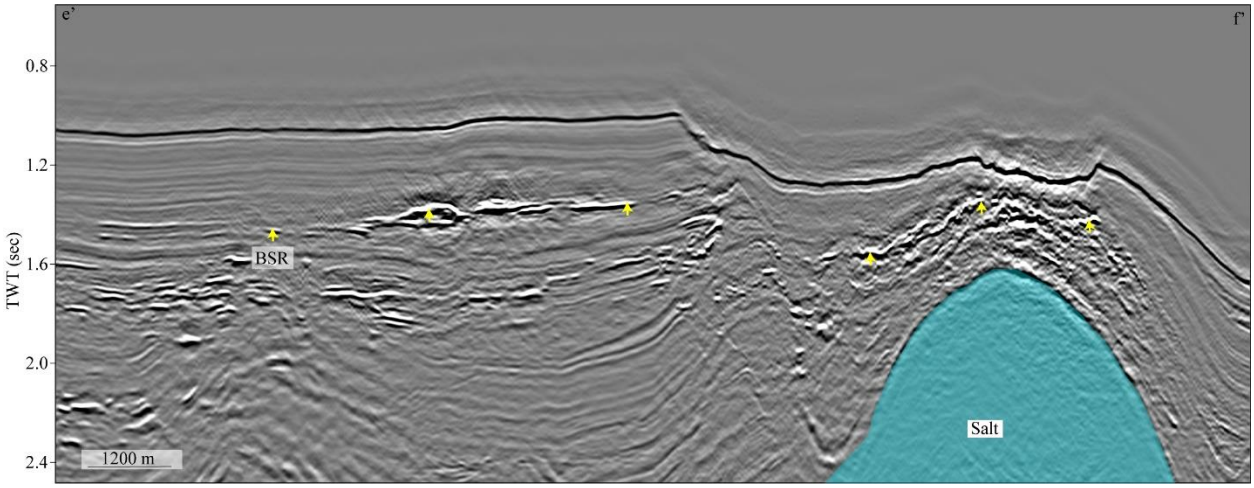

Figure 23: Seismic profile e'-f' showing a northwest-southeast cross-section across the eastern BSR system of Zone-3. The BSR is shown by the yellow arrows. The profile location is shown in Figure 18a.

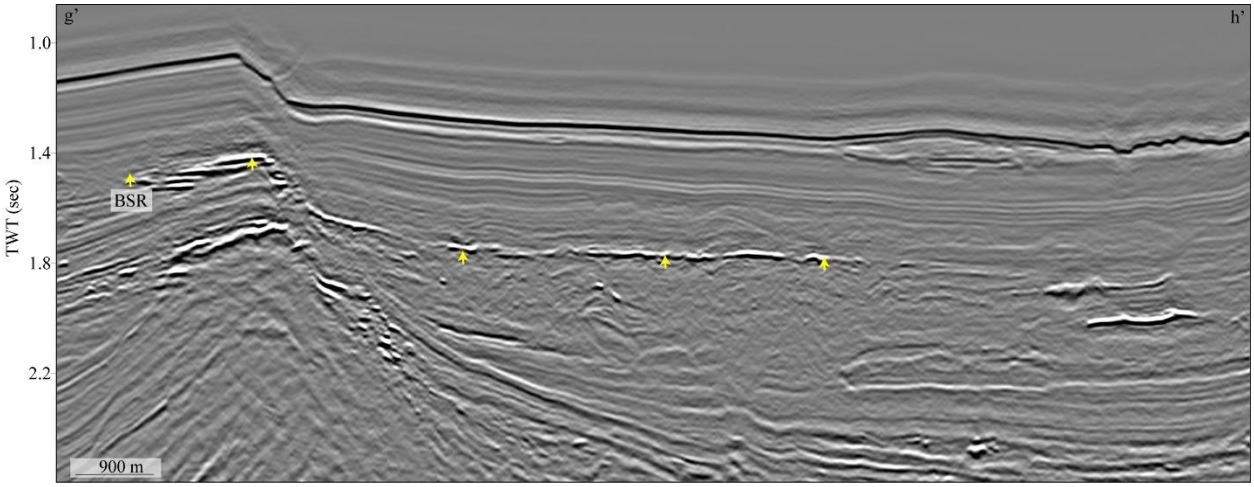

Figure 24: Seismic profile g'-h' showing a west-east cross-section across the eastern BSR system of Zone-3. The BSR is shown by the yellow arrows. The profile location is shown in Figure 18a.

4.4 Zone 4

Zone 4 is in the Garden Banks protraction area, with water depths from 850 m to 1000 m (Figure 2). Only one BSR system has been identified in Zone 4 (Figure 25) in seismic volume B-101-93-LA. This BSR was previously identified by BOEM, though the mapped areas do vary slightly between each interpretation (Figure 25).

The BSR system in Zone 4 is relatively small, covering an area of only 6 km^2. Figures 26 and 27 show this BSR in seismic profiles. This BSR system is located above salt and the depth of the BSR varies from 170 msec to 320 msec TWT below the seafloor, corresponding to depths of 140 m to 270 mbsf.

Based on the BSR, the estimated geothermal gradient in Zone 4 is 30-40 °C/km. There are no well logs available in close proximity to this specific BSR system.

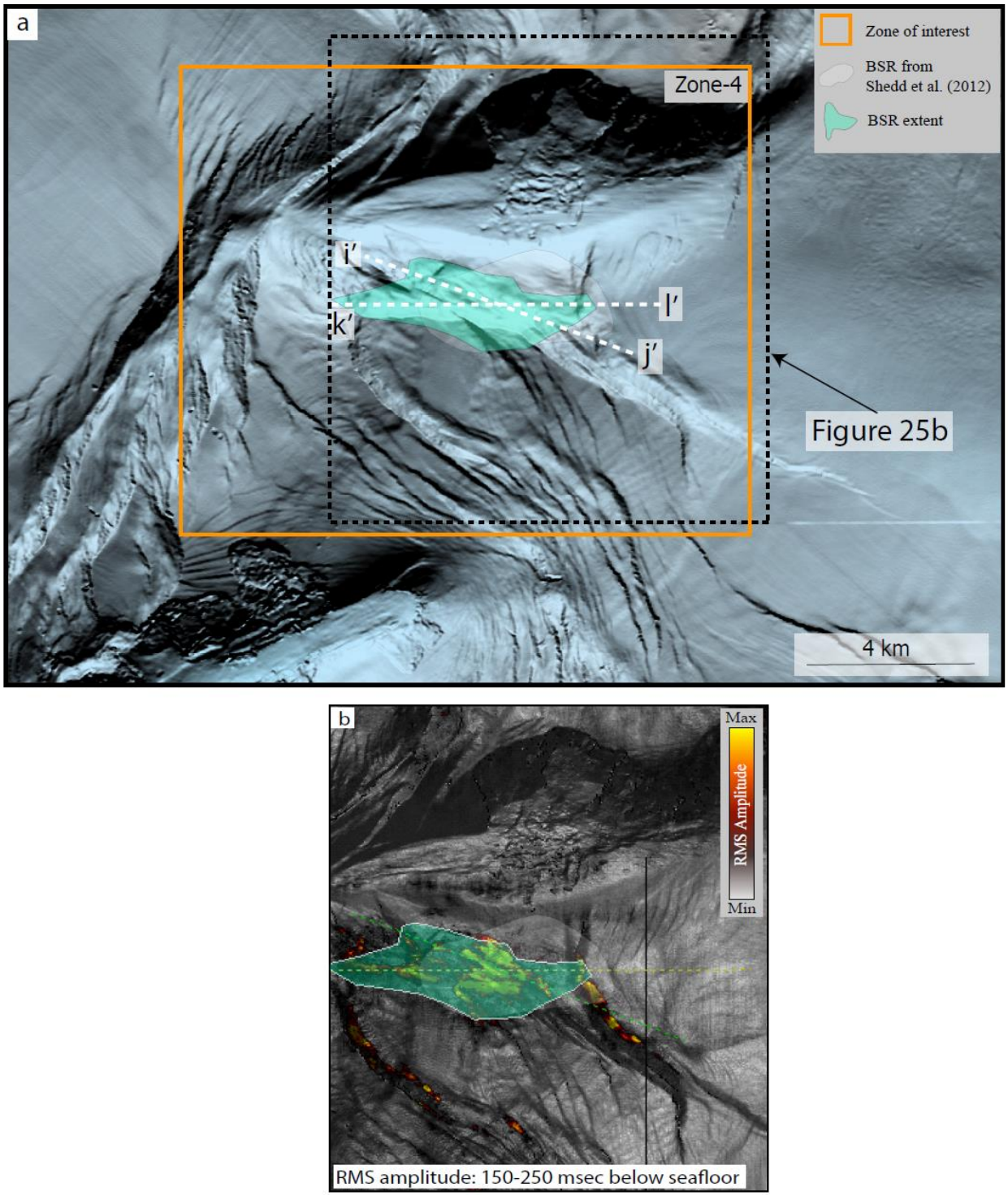

Figure 25: A bathymetric map showing the BSR extent within Zone-4 of Project Area 2.1 (Kramer and Shedd, 2017). *White dashed lines show the track of seismic profiles. b) An RMS amplitude map within 150 - 250 msec window below the seafloor highlights areas with elevated amplitudes*

corresponding to the BSR zones. The RMS amplitude map is generated using the seismic volume B-101-93-LA.

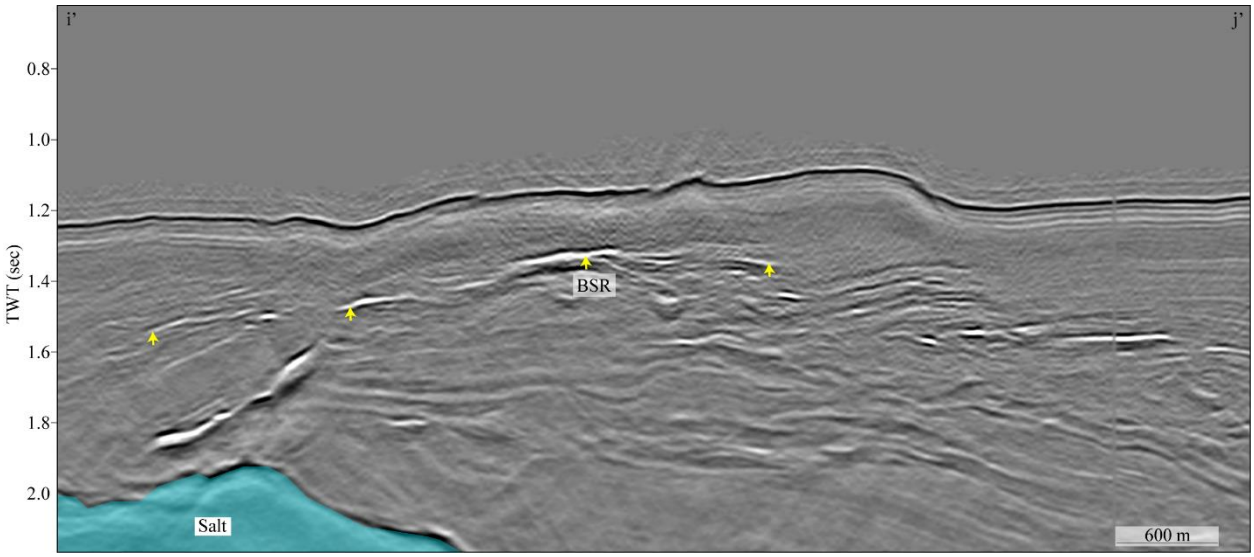

Figure 26: Seismic profile i'-j' showing a northwest-southeast cross-section across the BSR system of Zone-4. The BSR is shown by the yellow arrows. The profile location is shown in Figure 25a.

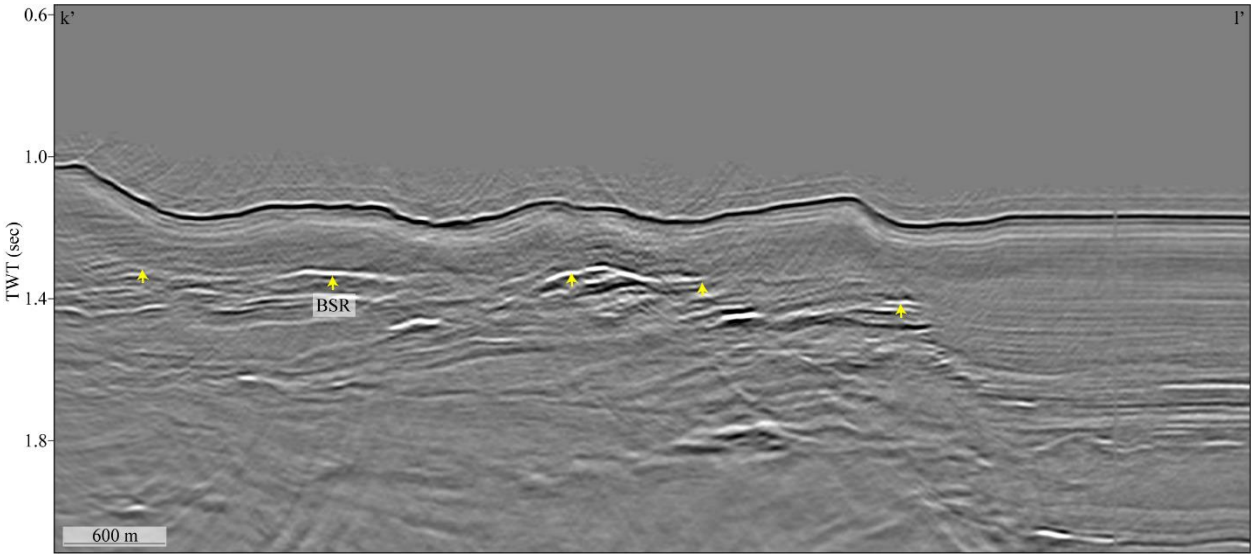

Figure 27: Seismic profile k'-l' showing a west-east cross-section across the BSR system of Zone-4. The BSR is shown by the yellow arrows. The profile location is shown in Figure 25a.

4.5 Zone 5

Zone 5 is situated within the Garden Banks protraction area (Figure 2). The water depth in this zone ranges between 700 m to 1200 m below sea level. In this zone, the only identified BSR was initially recognized by BOEM and further confirmed in this study, using the seismic volume B-101-93-LA (Figure 28). This BSR system covers an area of approximately 6 km^2 and is located above shallow doming salt.

Figures 29 and 30 show two seismic profiles across this BSR system. The BSR above the salt is quite shallow and deepens gradually away from the salt, ranging from 91 to 550 msec TWT (~77 m to ~475 m below the seafloor). The estimated geothermal gradient in this region has significant variation, with ~20 °C/km away from the salt and 65 °C/km above the salt.

No wells have been drilled near Zone 5 (Figure 2).

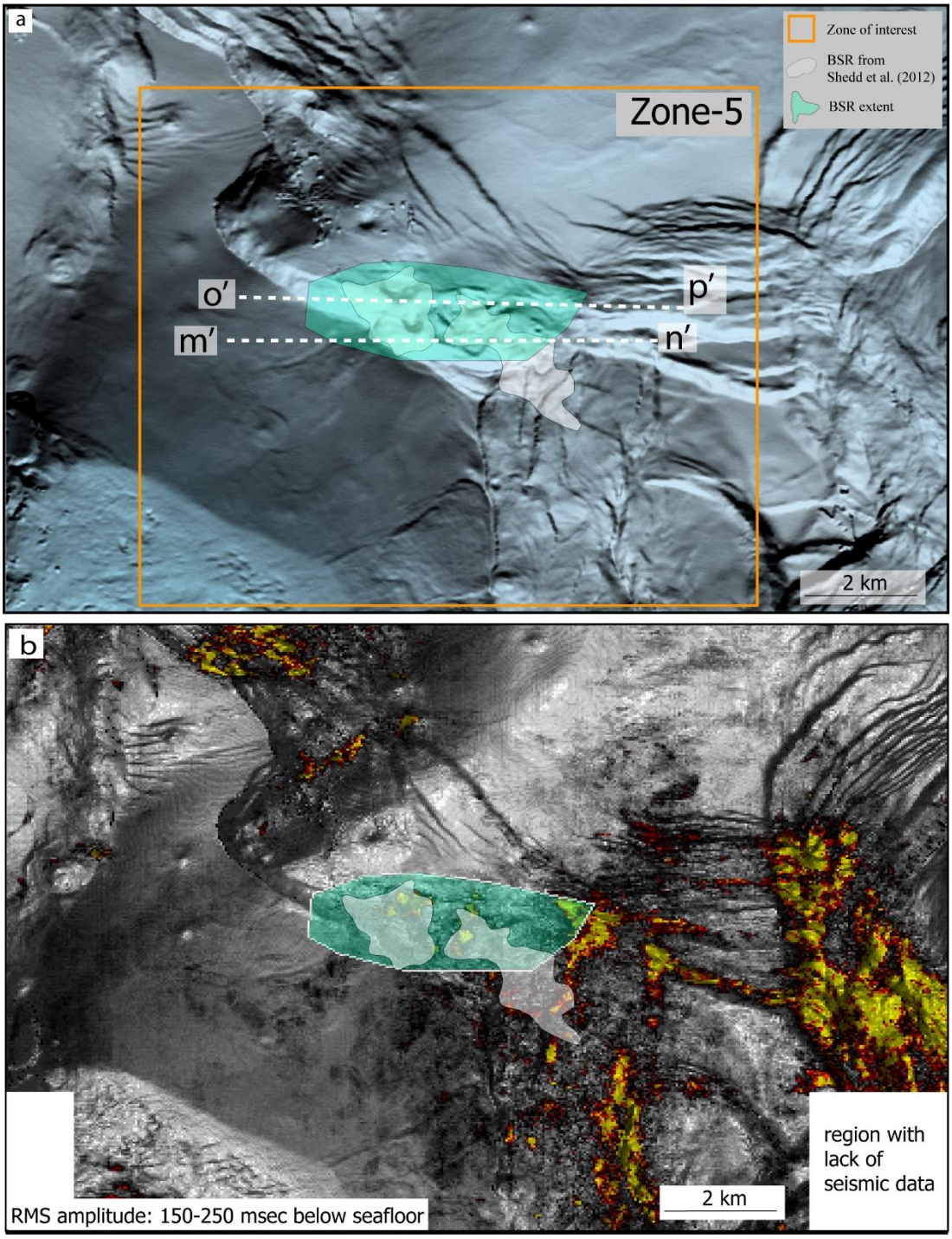

Figure 28: A bathymetry map showing the BSR extent within Zone-5 of Project Area 2.1 (Kramer and Shedd, 2017). *White dashed lines show the track of seismic profiles. b) An RMS amplitude map within 150 - 250 msec window below the seafloor highlights areas with elevated amplitudes corresponding to the BSR zones. The RMS amplitude map is generated using the seismic volume B-101-93-LA.*

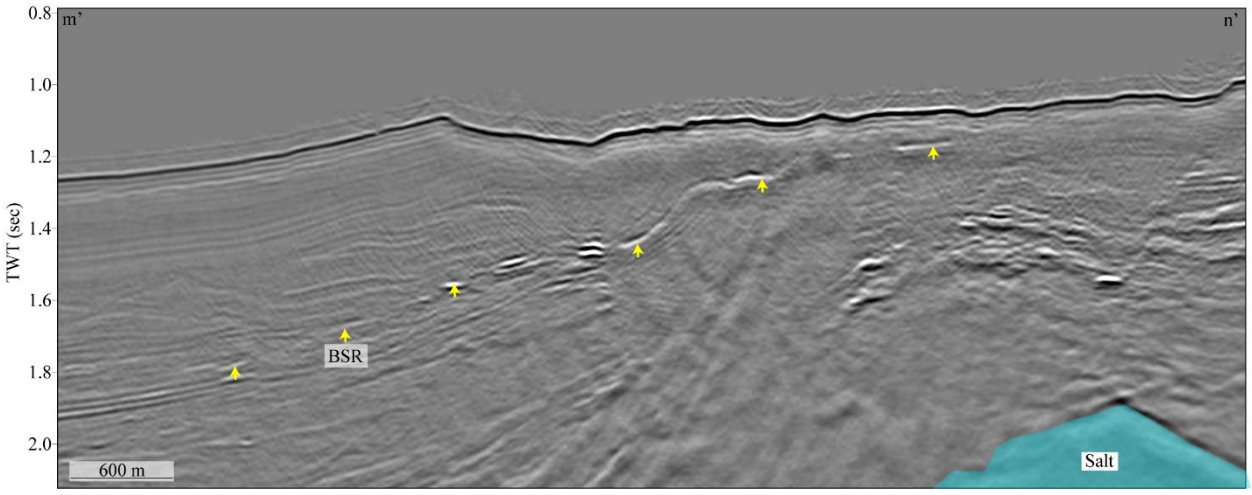

Figure 29: Seismic profile m'-n' showing a west-east cross-section across the BSR system in Zone-5. The BSR is shown by the yellow arrows. The profile location is shown in Figure 28a.

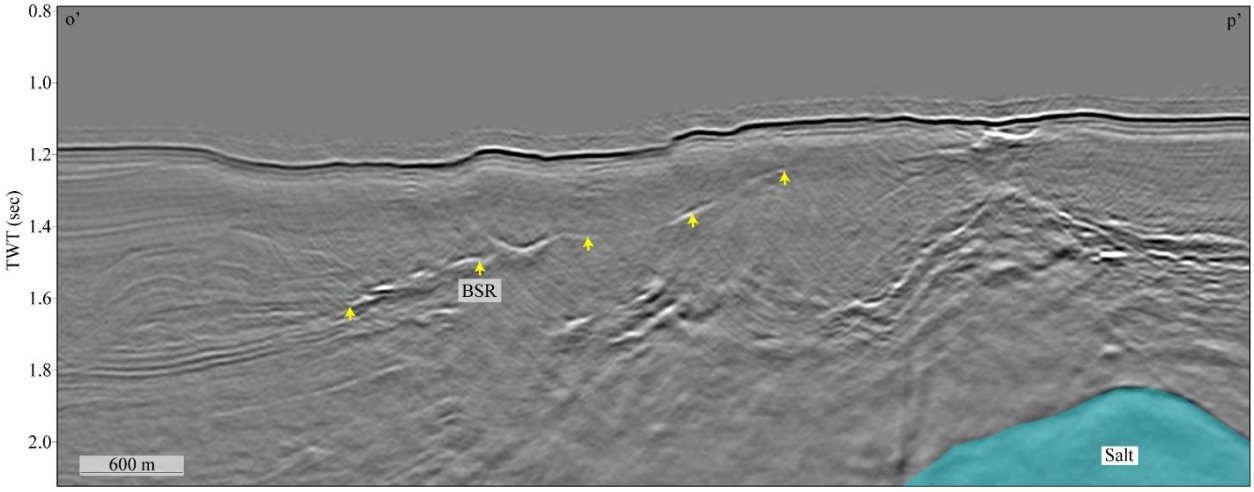

Figure 30: Seismic profile o'-p' showing a west-east cross-section across the BSR system in Zone-5. The BSR is shown by the yellow arrows. The profile location is shown in Figure 28a.

4.6 Zone 6

Zone 6, situated within the Garden Banks protraction area (Figure 2), has water depths ranging from 750 m to 1300 mbsf. Only one BSR system has been identified in this zone, which was originally mapped by BOEM (Figure 31). Seismic volume B-02b-97-LA was used to analyze this BSR system.

Covering a significant area of approximately 130 km^2, this BSR occurs from 200 msec to 530 msec TWT below seafloor, which corresponds to ~170 mbsf to 450 mbsf. Figures 32-34 show the BSR across this system. The BSR tends to be shallower above the salt layer, gradually increasing as it moves away from the salt, as depicted in Figures 32 and 34. A small clustered BSR is observed within this system (see Figures 32, and 34). This clustered BSR covers an area of approximately 2 km^2, as shown in Figure 31. We do not observe any peak-leading reflections in this area.

The BSR-derived geothermal gradients within this system demonstrate a range of 20 – 55 °C/km, with the highest values above the salt. The nearest well to this BSR system is API # 608074006500, located ~5 km north of the mapped BSR system, and has no data in shallow interval.

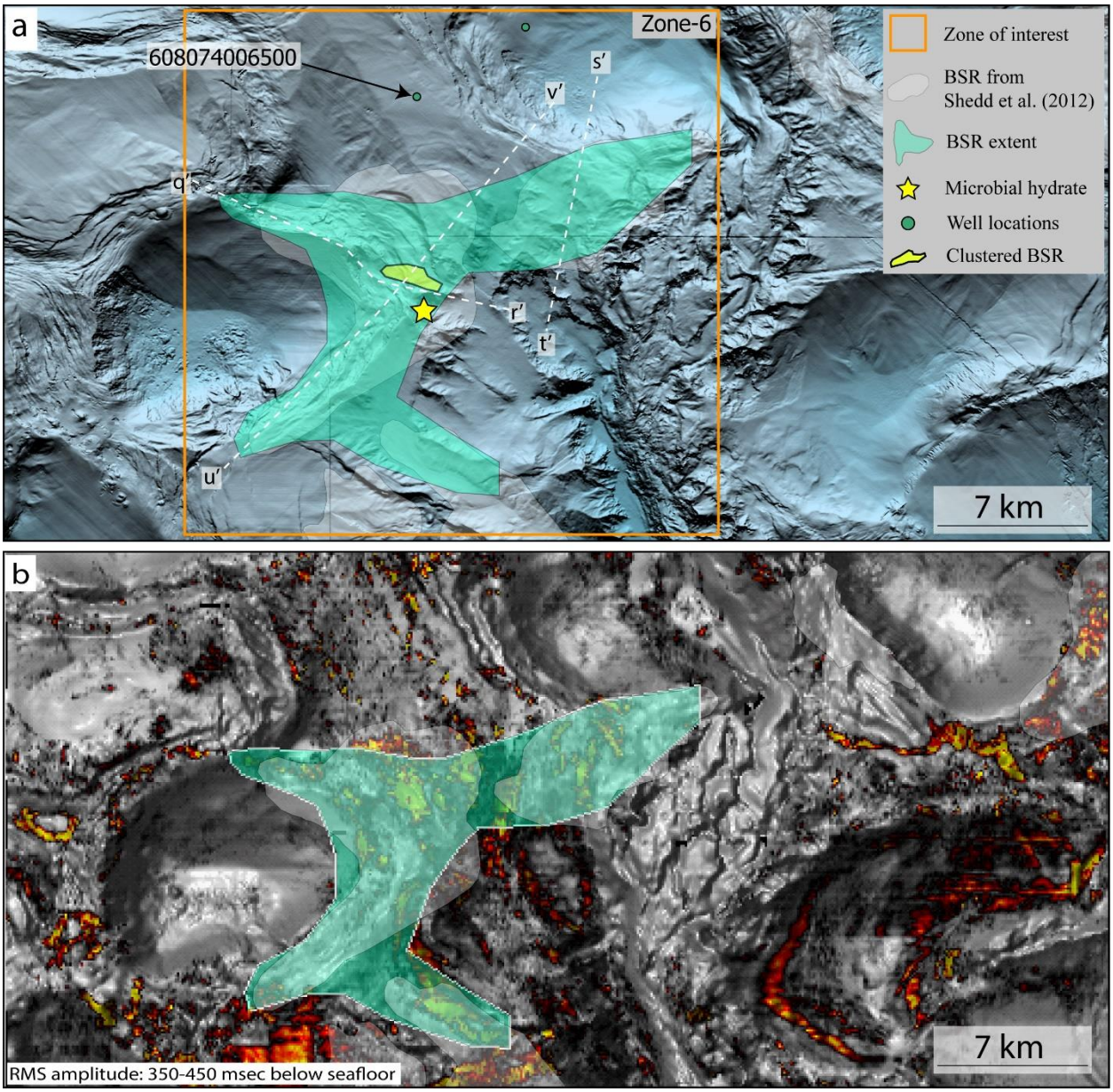

Figure 31: A bathymetry map showing the BSR extent within Zone-6 of Project Area 2.1 (Kramer and Shedd, 2017). *White dashed lines show the track of seismic profiles. b) An RMS amplitude map within 350 - 450 msec window below the seafloor highlights areas with elevated amplitudes corresponding to the BSR zones. The RMS amplitude map is generated using the seismic volume B-02b-97-LA.*

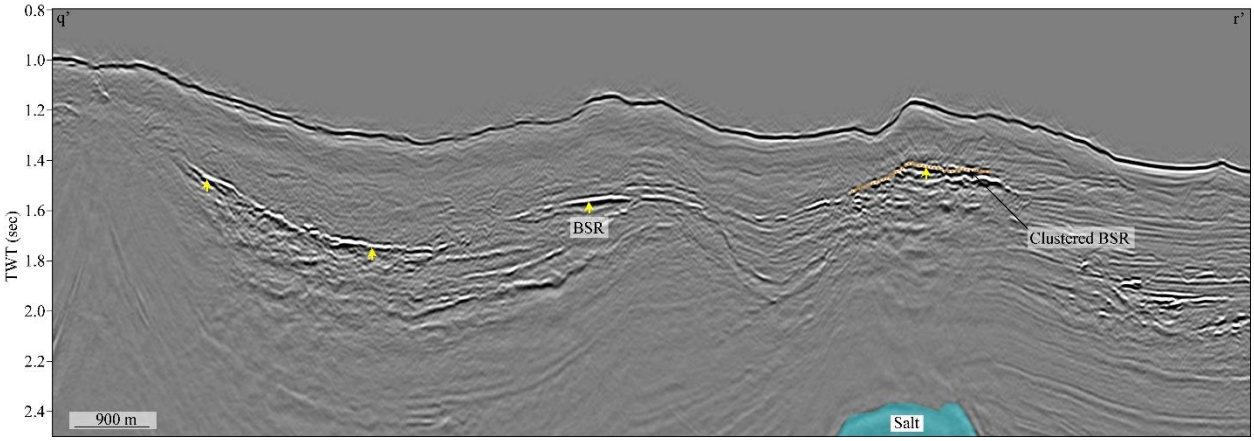

Figure 32: Seismic profile q' – r' showing cross-section of the BSR system of Zone-6. The BSR is shown by the yellow arrows. The profile location is shown in Figure 31a.

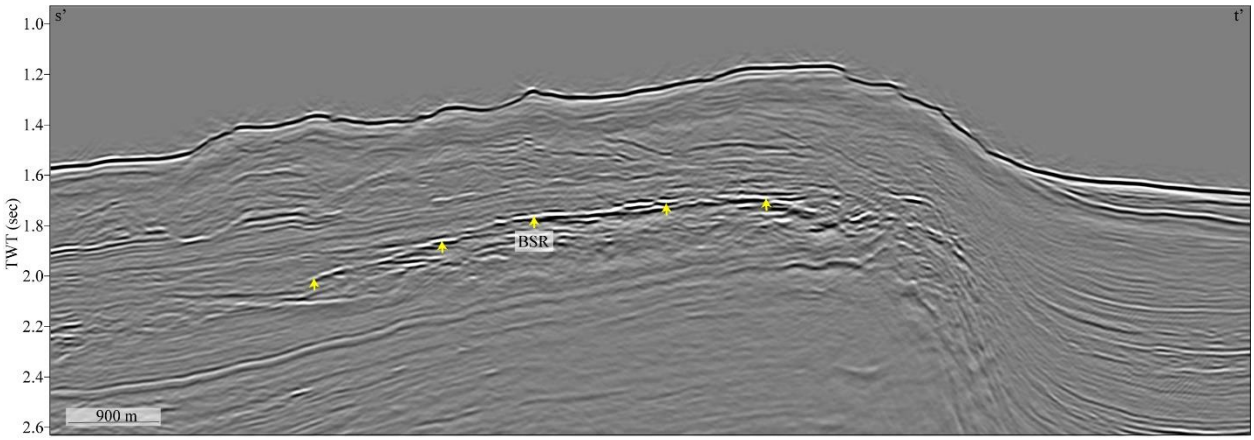

Figure 33: Seismic profile s'-t' showing a northeast-southwest cross-section across the BSR system of Zone-6. The BSR is shown by the yellow arrows. The profile location is shown in Figure 31a.

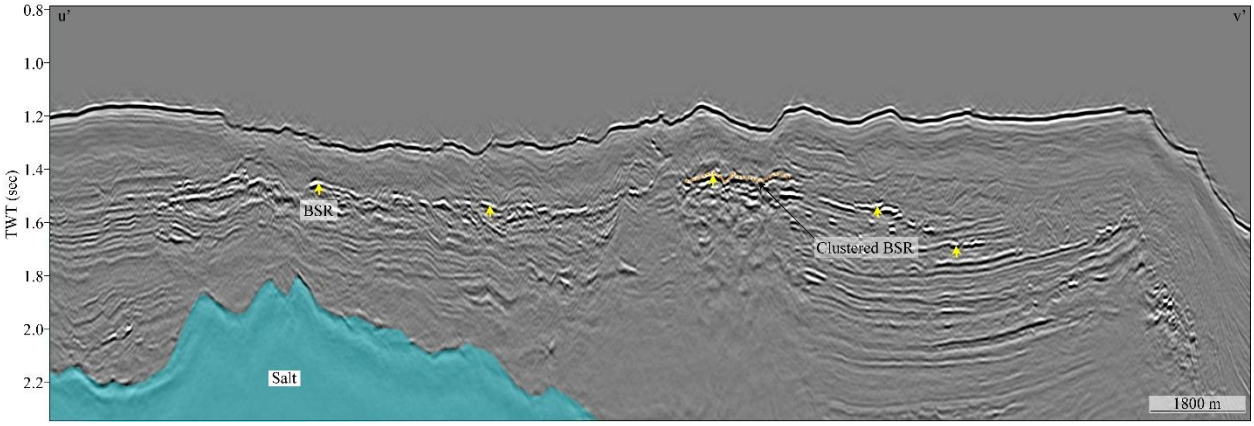

Figure 34: Seismic profile u'-v' showing a southwest-northeast cross-section across the BSR system of Zone-6. The BSR is shown by the yellow arrows. The profile location is shown in Figure 31.

5 Gas resource estimation

In previous reports, the hydrate resource estimate was based on the positive amplitude portion of phase reversals, which are considered a reliable indicators of hydrate presence (Boswell et al., 2012). However, in this specific project area, we did not observe any phase reversals. Consequently, we adopted an alternative approach where hydrate resources were estimated based on the presence of clustered BSRs.

Clustered BSRs may be indicative of potential gas hydrate accumulations, as they are often associated with structural environments that facilitate the migration of free gas to the hydrate stability zone. Previous studies in locations such as Green Canyon 955 (McConnell et al., 2010) and the Perdido hydrate system (Alamino Canyon 810, 856, and 857) (Portnov et al., 2019) in the Gulf of Mexico have estimated high gas hydrate saturation above clustered BSRs. However, two locations are not enough to establish a convincing trend, and moreover, neither of these sites have features or clear horizons within the hydrate stability zone that can be used to identify high saturation layers. Hence, estimates of hydrate resources based on clustered BSRs are certainly less reliable compared to those based on phase reversals in seismic data, resulting in lower confidence in their presence and volume. In the volumetric estimates provided below, we do not incorporate

a quantitative probability of success that the resources exist; in other words, the resource estimates represent an un-risked volume.

We determine both high and low estimates for gas hydrate accumulations by considering the total area covered by clustered BSRs. The low estimate is based on a 10 m-thick sand layer, 30% porosity, and 10% gas hydrate saturation. The high estimate assumes a 30 m-thick sand layer, 40% porosity and 75% gas hydrate saturation. Using this methodology, we do not generate a mean or expected resource volume, but instead present the range of resources as it may correspond to the distal fractiles of a stochastic or monte carlo approach. All reported resource volumes are conditional upon geologic success of finding gas hydrate.

Clustered BSR are found in Zones 2, 3, and 6 of Project Area 2.1, covering a total land area of 35 km^2 when combined (refer Figures 11, 18, and 31). This leads to minimum and maximum (un-risked) estimates for hydrate-bound free gas resources of 1.7 and 52 billion cubic meters (BCM), or 60 and 1800 billion cubic feet (bcf) respectively at standard temperature and pressure (STP). These estimates are much higher than previous estimates; this is certainly the result of the large area (35 km^2) that we are considering for these estimates. In other Project Areas, the extent of positive amplitude phase reversals is much smaller, though we have higher confidence of hydrate presence in areas with phase reversals.

6 Conclusion

We map ten BSRs in Project Area 2.1 that span a total area of ~ 700 km^2. These ten BSRs are divided into six zones (Figure 2). The BSR in Zone 1 is the largest that has been reported in the Gulf of Mexico. In Zone 1 sand intervals were identified above the BSR or the base of hydrate stability where modest increases in resistivity were observed in well log data. This increase in resistivity may indicate the presence of hydrate (Frye et al., 2010) or it could be simply a response to change in lithology (Cook and Tost, 2014).

Unlike other Project Areas, we do not observe phase reversals in Project Area 2.1.

We mapped the clustered BSRs in Zone-2, Zone-3, and Zone-6 of Project Area 2.1. The combined area covered by the clustered BSRs is approximately 35 km^2. By considering only clustered BSRs,

we estimate the volume of hydrate-bound free gas at STP in this area to be around 1.7 – 52 BCM. However, it is important to note that the confidence in this estimate is low due to uncertainty regarding the presence of hydrate at clustered BSRs, and no quantitative risk was applied in the volumetric estimate.

7 References

Bureau of Ocean Energy Management (2022). Retrieved November 25, 2022, from https://www.boem.gov/oil-gas-energy/mapping-and-data/map-gallery/northern-gom-deepwater-bathymetry-grid-3d-seismic.

Boswell, R., Collett, T.S., Frye, M., Shedd, W., McConnell, D.R., Shelander, D., 2012. Subsurface gas hydrates in the northern Gulf of Mexico. Mar. Pet. Geol. 34, 4–30. https://doi.org/10.1016/j.marpetgeo.2011.10.003

Collett, T.S., Ladd, J., 2000. Detection of gas hydrate with downhole logs and assessment of gas hydrate concentrations (saturations) and gas volumes on the Blake Ridge with electrical resistivity log data. Proc. Ocean Drill. Progr. Sci. Results 164, 179–191. https://doi.org/10.2973/odp.proc.sr.164.219.2000

Cook, A.E., Tost, B.C., 2014. Geophysical signatures for low porosity can mimic natural gas hydrate: An example from Alaminos Canyon, Gulf of Mexico. J. Geophys. Res. Solid Earth 119, 7458–7472. https://doi.org/10.1002/2014JB011342

Frye, M., Shedd, W.W., Godfriaux, P.D., Dufrene, R., Collett, T.S., Lee, M.W., Boswell, R., Jones, E., McConnell, D.R., Mrozewski, S., Guerin, G., Cook, A., 2010. Gulf of Mexico gas hydrate joint industry project leg II: Results from the Alaminos Canyon 21 Site. Proc. Annu. Offshore Technol. Conf. 2, 975–995. https://doi.org/10.4043/20552-ms

Hillman, J.I.T., Cook, A.E., Sawyer, D.E., Küçük, H.M., Goldberg, D.S., 2017. The character and amplitude of 'discontinuous' bottom-simulating reflections in marine seismic data. Earth Planet. Sci. Lett. 459, 157–169. https://doi.org/10.1016/j.epsl.2016.10.058

Kramer, K. V., Shedd, W.W., 2017. A 1.4-billion-pixel map of the Gulf of Mexico seafloor. Eos

(United States). https://doi.org/10.1029/2017eo073557

Portnov, A., Cook, A.E., 2020. Gulf of Mexico Hydrate Mapping and Interpretation Analysis. Bureau of Ocean Energy and Management.

Portnov, A., Cook, A.E., 2019. Gulf of Mexico Hydrate Mapping and Interpretation Analysis. Bureau of Ocean Energy and Management.

Portnov, A., Cook, A.E., Sawyer, D.E., Yang, C., Hillman, J.I.T., Waite, W.F., 2019. Clustered BSRs: Evidence for gas hydrate-bearing turbidite complexes in folded regions, example from the Perdido Fold Belt, northern Gulf of Mexico. Earth Planet. Sci. Lett. 528, 115843. https://doi.org/10.1016/j.epsl.2019.115843

Sassen, R., Losh, S.L., Cathles, L., Roberts, H.H., Whelan, J.K., Milkov, A. V., Sweet, S.T., DeFreitas, D.A., 2001. Massive vein-filling gas hydrate: Relation to ongoing gas migration from the deep subsurface in the Gulf of Mexico. Mar. Pet. Geol. 18, 551–560. https://doi.org/10.1016/S0264-8172(01)00014-9

Shedd, W., Boswell, R., Frye, M., Godfriaux, P., Kramer, K., 2012. Occurrence and nature of " bottom simulating reflectors" in the northern Gulf of Mexico. Mar. Pet. Geol. 34, 31–40. https://doi.org/10.1016/j.marpetgeo.2011.08.005

Skopec, S., Portnov, A., Cook, A.E., 2021. Gulf of Mexico Hydrate Mapping and Interpretation Analysis. Bureau of Ocean Energy and Management.

Triezenberg, P.J., Hart, P.E., Childs, J.R.C., 2016. National Archive of Marine Seismic Surveys (NAMSS): A USGS data website of marine seismic reflection data within the US Exclusive Economic Zone (EEZ).". US Geol. Surv. data release 10 F7930R7P.

Vanneste, M., De Batist, M., Golmshtok, A., Kremlev, A., Versteeg, W., 2001. Multi-frequency seismic study of gas hydrate-bearing sediments in Lake Baikal, Siberia. Mar. Geol. 172, 1–21. https://doi.org/10.1016/S0025-3227(00)00117-1